HHS Public Access

Author manuscript

Biomaterials. Author manuscript; available in PMC 2022 August 01.

Published in final edited form as:

Biomaterials. 2021 August ; 275: 120982. doi:10.1016/j.biomaterials.2021.120982.

Electrical stimulation of human neural stem cells via conductive polymer nerve guides enhances peripheral nerve recovery

Shang Song[1], **Kelly W. McConnell**[1], **Danielle Amores**[1], **Alexa Levinson**[1], **Hannes Vogel**[2], **Marco Quarta**[1,3,4], **Thomas A. Rando**[1,3,4], **Paul M. George**[1,5,*]

[1]Department of Neurology and Neurological Sciences, Stanford University School of Medicine, Stanford, CA, USA

[2]Department of Pathology, Stanford University, Stanford, CA, USA

[3]Paul F. Glenn Laboratories for the Biology of Aging, Stanford University School of Medicine, Stanford, CA, USA

[4]Center for Tissue Regeneration, Restoration and Repair, Veterans Affairs Hospital, Palo Alto, CA, USA

[5]Stanford Stroke Center and Stanford University School of Medicine, Stanford, CA, USA

Abstract

Severe peripheral nerve injuries often result in permanent loss of function of the affected limb. Current treatments are limited by their efficacy in supporting nerve regeneration and behavioral recovery. Here we demonstrate that electrical stimulation through conductive nerve guides (CNGs) enhances the efficacy of human neural progenitor cells (hNPCs) in treating a sciatic nerve transection in rats. Electrical stimulation strengthened the therapeutic potential of NPCs by upregulating gene expression of neurotrophic factors which are critical in augmenting synaptic remodeling, nerve regeneration, and myelination. Electrically-stimulated hNPC-containing CNGs are significantly more effective in improving sensory and motor functions starting at 1–2 weeks after treatment than either treatment alone. Electrophysiology and muscle assessment demonstrated successful re-innervation of the affected target muscles in this group. Furthermore,

*Corresponding author: Paul M. George, MD, PhD, Assistant Professor, Department Neurology and Neurological Sciences, 300 Pasteur Dr., MC5778, Stanford Stroke Center, School of Medicine, Stanford University, Stanford, CA 94305-5778, Tel: +1 (650) 725-0013, pgeorge1@stanford.edu.

Credit Author Statement

Author contributions: SS designed, performed, and supervised all the experiments reported, analyzed the data, and wrote the manuscript. KM performed the experiments for immunostaining and collected data for immunostaining and histological stains and performed the behavior testing. DA assisted with animal surgeries. AL assisted with animal surgeries and behavior testing. HV provided advice and design of histological experiments and their interpretation. MQ and TAR provided advice, experimental design, and equipment for the gripping test. PMG contributed to design of all experiments, analyzed data and wrote the manuscript.

Declaration of interests

The authors declare that they have no known competing financial interests or personal relationships that could have appeared to influence the work reported in this paper.

The authors declare the following financial interests/personal relationships which may be considered as potential competing interests:

Competing interests: The authors declare no competing financial interests.

histological analysis highlighted an increased number of regenerated nerve fibers with thicker myelination in electrically-stimulated hNPC-containing CNGs. The elevated expression of tyrosine kinase receptors (Trk) receptors, known to bind to neurotrophic factors, indicated the long-lasting effect from electrical stimulation on nerve regeneration and distal nerve re-innervation. These data suggest that electrically-enhanced stem cell-based therapy provides a regenerative rehabilitative approach to promote peripheral nerve regeneration and functional recovery.

Keywords

Electrical stimulation; Stem cells; Nerve repair; Conductive polymer; Functional recovery

1. Introduction

Peripheral nerve injury (PNI) leads to sustained nerve damage in pediatric and adult populations as the result of motor vehicle accidents, combat trauma, as well as neoplastic, vascular, and compression disorders[1,2]. The fundamental challenge of successful peripheral nerve recovery is inadequate functional outcomes as nerves slowly regenerate[3,4]. The prolonged peripheral nerve regeneration delays the re-innervation process of muscle and other sensory organs, which leads to poor functional recovery[5,6]. The current autograft treatments are limited by the availability of donor nerves in terms of length and size and require an additional surgical procedure with significant morbidity at the donor site. Alternatively, synthetic nerve grafts have been studied, but they lack the regenerative potential[7] that optimally supports appropriate nerve regeneration and functional recovery.

Stem cell transplantation promotes nerve regeneration and recovery in treating PNI when supported with either natural (e.g. collagen)[8,9] or synthetic (e.g. poly(D,L-lactic acid), poly-epsilon-caprolactone, silicone tube)[10–13] conduits. Bioengineering techniques, such as microinjection[14], 3D printing[15–17], and chemical exfoliation[18] and vapor deposition[19] have been used to shape biomaterials to provide structural and biochemical platforms for cellular activities and axonal guidance. However, the optimal microenvironment for human neural progenitor cells (hNPCs) to support their regenerative potential has yet to be achieved. One main mechanism through which hNPCs improve peripheral nerve regeneration is through their ability to produce neurotrophic factors, such as brain-derived neurotrophic factor (BDNF), that promote axonal regeneration and increase the level of myelination[20,21]. The secreted BDNF in various forms have the ability to bind receptors such as the tropomyosin receptor kinase (Trk)[22,23]. The activation of these pathways increases the actin transport and accumulation and stimulates growth cone sprouting during the nerve repair process[24,25]. Therefore, these neurotrophic factors are important in cell fate regulation, axon outgrowth, dendrite pruning, and neuronal function patterning and innervation that are crucial for the development of the nervous systems[26–30]. Hence, the ability to manipulate the hNPCs' microenvironment to secrete bioactive neurotrophic molecules is a critical step in enhancing the regenerative potential of nerve guides for better neural cell survival and regeneration.

Conductive polymers have garnered interest because of the ability to control electrical properties of the regenerative environment[31–35]. Particularly, polypyrrole (PPy) is one of most commonly studied conductive biomaterials. PPy is known for its high conductivity under physiological conditions and excellent biocompatibility *in vivo*[32–34,36]. PPy can be fabricated with different mechanical and electrical properties by altering its synthesis conditions (e.g. temperature, doping agents and solvents)[33]. Unlike previous synthetic nerve guides that are solely designed for structural support, nerve guides made of conductive polymers allow for the further investigation of the electrical effects on stem cells and the interactive roles of electrical stimulation and stem cells in treating peripheral nerve injuries. More specifically, the conductive polymer nerve guides in this study allow *in vivo* electrical stimulation to be applied to transplanted stem cells postoperatively to optimize the regenerative environment.

Here, we have engineered conductive nerve guides (CNGs) made of PPy that allow direct electrical manipulation of hNPCs after implantation to enhance their therapeutic potential for peripheral nerve recovery. To understand the electrical effect on hNPCs, we first studied *in vitro* stimulated hNPC-containing CNGs which showed upregulated gene expression of multiple neurotrophic factors. Because these neurotrophic factors are known to be important in enhancing axon regeneration and myelination[20,21,26–30], we applied electrical stimulation post hNPC transplantation via CNGs in the rat sciatic nerve transection model to investigate their potential impact on peripheral nerve regeneration and functional recovery. This conductive nerve guide platform allows post-operative manipulation of electrical stimulation to encapsulated stem cells *in vivo*. Using a comprehensive assessment consisted of weekly animal functional tests, electrophysiology, and immunostaining analysis, we found that electrically-stimulated hNPCs significantly promoted peripheral nerve regeneration and functional recovery in rats. The electrically-stimulated hNPCs led to the regeneration of more myelinated nerve fibers with improved electrical properties while restoring a substantial amount of muscle mass. As a result, these pathological changes greatly improved the ultimate functional recovery. Additionally, regenerated nerve segments from electrically-stimulated stem cells showed upregulated tyrosine kinase receptors (Trk) which are known to bind with high affinity and specificity to neurotrophic factors[37,38]. In summary, our results highlight the beneficial effect of using electrical stimulation to enhance the therapeutic potential of stem cell therapy that may offer new treatment strategies for PNI in the clinical setting.

2. Materials and methods

2.1 Fabrication of conductive nerve guides

The 0.2M PPy solution was doped with 0.2M sodium dodecylbenzenesulfonate (NaDBS) which was then electroplated onto a 14G Nickel-Chromium Alloy wire at 2mA/cm^2 for 2 hours as previously described[32,36,39] (Fig. 1a). The electroplated PPy tubes were gently detached with the following dimensions: 1.63mm inner diameter and 15mm length. Wires were then attached to the ends of PPy tubes to allow for electrical stimulation. All conductive nerve guides and wires were immersed in water and electrically insulated with

non-conductive polyolefin and epoxy adhesive (1VAL8, Grainger) (Fig. 1b). They were sterilized under UV light prior to use.

2.2 Cell culture

hNP1 Neural Progenitor cells (hNPCs) (ArunA Biomedical) derived from WA09 hESCs were cultured in Matrigel™ (BD Bioscience) coated tissue culture dishes. Cells were maintained in complete neural expansion medium composed of AB2™ medium supplemented with 1× ANS™ (ArunA Biomedical Inc.), 20 ng/mL Leukemia Inhibitory Factor (LIF, Millipore), 2 mM L-Glutamine, 20 ng/mL basal human fibroblast growth factor (bFGF, Millipore) at 37 °C and 5% CO_2. Culture medium was changed every other day and hNP1 cells were passaged every 3–4 days by manual pipetting.

2.3 Electrically-stimulation of cell-seeded conductive nerve guides

Prior to cell seeding on conductive scaffolds, 1 million hNPCs were encapsulated in 1% alginate solution. Then 40 μL of hydrogel-immobilized cell solution was encapsulated into the conductive nerve guide. The cross-linked solution containing 1%$CaCl_2$ was added to all scaffolds and replaced with fresh medium culture under standard culture conditions. New medium was added to all conditions the next day. The cell-seeded conductive nerve guides were electrically stimulated to achieve a uniform electric field strength (40 V/m at 100 Hz) based on Electromagnetic Finite Element Method (FEM) simulation[39]. The uniform electric field strength was calculated on ANSYS HFSS using the FEM solver with the model subdivided into many small subsections in the form of tetrahedra as described previously[39]. The electric field was computed based on experimental measurements from scaffold physical dimensions, material electrical properties, and stimulation parameters (i.e. electrical resistivity of connection ~0.007 Ωcm). Specifically, physical dimensions of scaffolds were measured by a caliper. The experimental conductivity was measured to be 7.65 ± 0.95 S/cm (n=4) using the direct current (d.c.) four-point probe method with a Keithley 2400 Source Meter 45 at room temperature. The electrical parameters that resulted in this uniform electric field included a 10ms square pulse wavelength with ± 400mV at 100 Hz for 1 hour. After a 1-hr stimulation, all samples were incubated for 24 hours before analysis. The optimization of these electrical parameters (40 V/m at 100 Hz for 1 hour) was demonstrated in our supplemental data, in which different parameters of stimulation through conductive CNGs were tested to find the optimal upregulation of neurotrophic factors without affecting cell viability (Supplementary Fig. 1 and 2).

2.4 Cell viability

For the lactate dehydrogenase (LDH) (Pierce, Thermo Fisher Scientific) assay, the positive control was a sample medium collected from cells that were lysed with a buffer reagent provided by the manufacturer. The negative control was medium from cells cultured on a tissue culture plate under standard culture conditions. The supernatant from unstimulated and stimulated cell-seeded conductive nerve guides were also collected. The supernatant from all conditions was then mixed with the reaction mixture and later added with the stop solution. The LDH activity was measured by the Spectra Max M2 plate reader (Molecular Devices) at an absorbance of 490nm and 680nm based on the manufacturer's protocol. For the live/dead staining, a viability kit (L3224, Thermo Fisher Scientific) was used per the

manufacturer's protocol. The cell-seeded conductive nerve guides were sectioned and incubated with the staining solution. Samples were subsequently imaged under the Keyence BZ-X710 microscope.

2.5 Quantitative gene expression

The quantitative real-time polymerase chain reaction (qRT-PCR) was performed using the RNeasy Mini Kit (Qiagen) based on the manufacturer's protocol. The iScript cDNA Synthesis Kit (Bio-Rad) was used for cDNA synthesis. The QuantStudio 6 Flex Real-Time PCR System (Thermo Fisher Scientific) was used to perform quantitative real-time PCR. Taq polymerase and Taqman primers (Thermo Fisher Scientific) glyceraldehyde-3-phosphate dehydrogenase (*GAPDH* Hs02786624_g1), heparin binding EGF like growth factor (*HBEGF* Hs00181813_m1), vascular endothelial growth factor A (*VEGF-A* Hs00900055_m1), brain derived neurotrophic factor (*BDNF* Hs02718934_s1), and neurotrophin 3 (*NTF3* Hs00267375_s1) was used in the PCR reaction mixtures. The Delta-Delta CT method was utilized for analysis with the *GAPDH* housekeeping gene and hNPCs on tissue culture wells as references.

2.6 Implantation and electrical stimulation of conductive nerve guides *in vivo*

All procedures involving implantation and harvesting of electrodes on rat sciatic nerves were performed in accordance with protocols approved by the Institutional Animal Care and Use Committee (IACUC) at Stanford University. Surgical procedures were described by previously published protocols[36] with some modifications. The immunodeficient RNU rats (7–8 weeks, NCI-Frederick) were given buprenorphine 0.1 mg/kg intramuscularly before anesthesia and then anesthetized with 2% isoflurane in balanced oxygen. Under sterile conditions with external body warming, a 3-cm incision was made on the left thigh. An approximate 10mm transection of the sciatic nerve proximal to the tibial and peroneal bifurcation was performed. The conductive nerve guides were secured with 9–0 suture to bridge the nerve gap. Both ends of the nerve guides were inserted with a 2.5mm-long nerve; leaving 10 mm for the nerve to re-grow. Muscle layers were closed leaving the nerve guide wires unaffected. Wires were then hidden under the skins which were closed with Michel clips. In the case of electrical stimulation, wires were retrieved under the skin for direct stimulation of animals under anesthesia. Because wires were kept at sufficient length under the skin, no tension or pulling was exerted on the implants. In all experiments, CNGs and their attached wires were electrically insulated so that the electrical stimulation was specifically delivered to the implants and the transected nerve, reducing the possibility of stimulation of existing networks and induction of plasticity of nearby tissues. The exact same procedure minus the electrical stimulation was performed for the control animals without stimulation. Animals in the electrical stimulation groups received electrical stimulation on day 1, 3, and 5 with the same *in vitro* stimulation parameters (40 V/m at 100 Hz for 1 hour). The condition of general anesthesia was kept the same both in surgery and during electrical stimulation. All conductive regions of the nerve guides and wires are electrically insulated (Fig. 1b) as described in the section of fabrication of conductive nerve guides to restrict stimulation to the conductive nerve guides. Cells were seeded into conductive nerve guides 1 day prior to the implantation. Contralateral sides of the animals were used as healthy controls. Animals were fed with antibiotic water for 1 week after the

surgery. At the end of 12 weeks, animals were euthanized with carbon dioxide gas, fixed with whole animal perfusion, and followed by a secondary confirmatory of death for proper disposal. All nerve guides and gastrocnemius muscles were harvested during this process.

2.7 Animal behavior analysis

Animals were divided into matched groups and behavioral testing was performed by blinded individuals. Animals were trained on 3 separate days prior to recording the baseline behavior. After the implantation, weekly behavioral testing such as thermal nociception, extensor postural thrust and positional placing was assessed based on previously published protocols . *Thermal nociception* was assessed using a hot plate where hind paws were exposed to a temperature of 56°C, and the time (thermal latency) that the animal left its paw was measured with a stopwatch. The paw was removed by the experimenter after 12s to prevent injury to the animal or the development of hyperalgesia. Although the sensation of the lateral foot is mediated by the sciatic nerve, the hip and knee flexion necessary to remove the foot from the hot plate is mediated by the femoral nerve. Therefore, this test was specific for a nociceptive block. *Extensor postural thrust* measures the maximum weight that the rat could bear without its ankle touching the balance. The rat was held with its posterior placed above a digital balance on which it could bear weight with one hind paw at a time. *Positional placing response* was used to measure proprioception. A prone rat will respond to having its hind paw pulled back with the dorsum in contact with the table surface by returning it to a position alongside its flank: with the claws splayed (score = 1), severe defects result in the limb trailing behind the rat with the claws clubbed (score = 4). If the foot is returned fully to the flank but the digits are clubbed, the score is 2. Any other outcome (e.g., the foot is left out at an angle) yielded a score of 3. *Grip strength test* was used to quantify the muscular strength at the end of week 12. Briefly, the grip strength meter (Bioseb, Chaville, France) was positioned horizontally, and animals were held by the tail and lowered towards the apparatus. Rats were allowed to grab the metal grid and were then pulled backward in the horizontal plane. The force applied to the grid just before it loses grip was recorded as the peak tension.

2.8 Electrophysiology

Electrophysiology was conducted at the end of 12 weeks to collect the electrical signals from various experimental groups based on previously published protocols with modifications[41,42]. Animals were anesthetized with 2% isoflurane in balanced oxygen under sterile and body-temperature warming conditions. The stimulating electrodes were inserted into the proximal side of the sciatic nerve before the conductive nerve guide. The electrodes were connected to the external stimulator (33210A, Keysight). The recording electrodes were placed on the outside paw of the stimulated leg. The amplifier gain was set at 1,000 with the output of the amplifiers bandpass filtered at 300 Hz −10 kHz. The amplified potentials were recorded using the Labchart (Powerlab, AD Instrument). Stimuli were delivered in the form of constant voltage pulses with intensity from 300mV and every 1 s to gradually elicit nerve responses. Compounded action potential was continuously recorded before and after the stimulation, and the responses were saved to data files. The distance between the stimulating and the recording electrodes was measured. The conduction velocity, voltage amplitude, and latency were calculated based on previously

published method(52, 69). Specifically, conduction velocity was calculated using stimulation-recording distance divided by artifact-to-CAP (compound action potential) latency.

2.9 Histological staining

Harvested samples were processed based on the previous protocol[36]. Briefly, samples were fixed in a PBS solution with 4wt% formaldehyde. Regenerated nerves were isolated by manually removing the nerve guides under a surgical microscope. Harvested nerves were then embedded in paraffin and sectioned into 4 μm thickness. After deparaffinization, endogenous peroxidase was blocked with 3% hydrogen peroxide. Antigen retrieval was performed using Antigen Target Retrieval Solution (pH6) (Agilent Technologies, Santa Clara, CA, USA) heated to 100 °C for 10 min. Briefly, for Haematoxylin and Eosin (H&E) staining, samples were hydrated and stained with hematoxylin and eosin followed with extensive water washes. All of these steps were followed by dehydration in graded ethanol to xylene. Glass coverslips were applied using a resinous mounting medium (Thermo Scientific, Pittsburgh, PA). For the toluidine blue staining, samples were embedded in epoxy resin that were sectioned to 1–2 μm in 1% solution of toluidine blue. The number of fibers, myelin sheath thickness, and G-ratio (inner diameter vs. outer diameter of nerve fibers) were quantified using FIJI software. All staining quantification was performed double-blinded.

2.10 Immunofluorescent staining

After deparaffinization as described in the histological staining section, samples were immunofluorescent stained for neurofilament (NF), S100, pan Trk (including TrkA, TrkB, TrkC), and human nuclear membrane (Human Nuc). The slides were permeabilized for 10 minutes with tris-buffered saline (TBS: 93362, Sigma Life Science) with .025% TritonX-100 (T8787, Sigma Life Science) and then blocked with 10% Normal Goat Serum (NGS: 31873 Invitrogen) with 1% Bovine serum albumin (BSA: BP9706, Fisher BioReagents) in TBS for 2 hours at room temperature. The slides were incubated with primary antibodies diluted 1:100 – 1:250 in TBS with 1% BSA overnight at 4°C (NF: ab7795, S100ß: ab52642, TRK: ab181560, Abcam; Human Nuc: MA1–7628, Thermo Fisher Scientific). The slides were rinsed for 5 minutes with TBS with .025% TritonX-100 twice. The secondary antibodies (Alexa Fluor 555: A-21422, Alexa Fluor 488: A-11008; Thermo Fisher Scientific) were applied at a 1:100 concentration in TBS with 1% BSA for two hours at room temperature. The slides were washed again for five minutes three times with TBS. The nuclei were stained with DAPI (1:1000, D9542, Sigma-Aldrich) in TBS for 15 minutes at room temperature. The slides were washed a final time for five minutes in DI water, then dried and mounted with coverslips. The slides were imaged using the Keyence BZ-X710 microscope equipped with full BZ acquisition and analysis software. All staining quantification was performed blinded. The fluorescent intensity of the stains was quantified using FIJI to calculate the area fraction of the fluorescence.

2.11 Statistical analysis

G-ratio was calculated based on the ratio of inner and outer axonal diameters, which was then categorized into frequency bin. A polynomial trendline was adjusted to the histogram to indicate changes in frequency occurrence. The linear regression of the g-ratio measurement

was fitted to explain the variability of g-ratio around different axonal diameters. The R-squared value was a statistical measurement of how close samples are to the average linear regression line. Sample pairs were analyzed using the Student's t-test. Multiple samples were evaluated with one-way or two-way analysis of variance (ANOVA) followed by Tukey and multiple comparisons using GraphPad Prism software (San Diego, CA). A p value of <0.05 was accepted as statistically significant for all analyses. Data are presented as mean ± SE.

3. Results

3.1 Electrical stimulation enhances hNPC expression of key nerve repair factors *in vitro*

With the goal of developing an electrically-stimulated stem cell therapy capable of ameliorating peripheral nerve deficits, we first evaluated the effect of three dimensional (3D) electrical stimulation on hNPCs *in vitro*. We fabricated smooth CNGs with externally attached wires for encapsulation and electrical stimulation of hNPCs (Fig. 1a,b). Cells were immobilized in alginate hydrogel inside the CNGs so there was no direct topographical stimulation. To optimize the electrical stimulation pattern, we tested the effect of electrical stimulation on hNPCs in the CNGs across several stimulation parameters and durations (Supplementary Fig. 1 and 2)[39]. From these studies, we determined that a uniform electrical field strength of 40 V/m at 100 Hz for 1 hour was the optimal stimulation parameters compared to other stimulation conditions given the increased neurotrophic factor gene expression and unchanged cell viability. The resulted electrical field was calculated based on Electromagnetic Finite Element Method (FEM) simulation with experimental inputs measured from material properties and electrical stimulation parameters[39] (see section 2.3). To further assess viability of using 40 V/m at 100 Hz for 1 hour, the one-hour electrical stimulation did not significantly change the viability of hNPCs based on a lactate dehydrogenase (LDH) assay and live/dead staining after one day. The LDH assay demonstrated that the percentage of dead cells was 8.2±2.1% and 7.2±2.3% for unstimulated and stimulated hNPCs in the CNGs, respectively (Fig. 1c). The cross-section images of both conditions presented highly viable hNPCs immobilized in the CNGs (Fig. 1c). These studies demonstrate the feasibility of culturing and electrically stimulating hNPCs in the CNGs with no change in their cell survival. In fact, stimulated hNPC-containing CNGs showed an increase in viability compared to the unstimulated condition with live/dead staining (Supplementary Fig. 3).

Previous studies that directly introduced hNPCs into the nerve defects demonstrated that stem-cell released neurotrophic factors are important in regulating axonal growth and myelination[44,45]. To investigate this in our system, we evaluated how neurotrophic factors differed in their gene expression between unstimulated and stimulated hNPC-containing CNGs. We specifically screened important trophic factors in the peripheral nervous system including vascular endothelial growth factor-A (VEGF-A), brain-derived neurotrophic factor (BDNF), neurotrophin-3 (NTF-3), and heparin-binding EGF like growth factor (HBEGF). VEGF-A has been demonstrated to be critical in angiogenesis, cell proliferation, and neural plasticity[32,46,47]. Increased VEGF-A expression in hNPCs was observed on 2D PPy film under electrical stimulation of 2V at 1kHz for one hour[32]. Applied electric fields of small

physiological magnitude (75–100 V/m) was also shown to direct cellular reorientation, elongation, migration, and signaling activation through the VEGF pathway[46]. BDNF and NTF-3 were examined because they are crucial in growth support, differentiation, and neuron survival in the development, maintenance, and regeneration of the nervous systems[26–30]. Direct stimulation (50–1000 V/m) enhanced BDNF level on rat Schwann cells through PPy and chitosan composite *in vitro*[48]. Low levels of electrical stimulation were found to increase the proliferation of neural precursor cells and upregulated their EGF expression in the rat brains[49]. In our study, the gene expression of VEGF-A, BDNF, and NTF-3 significantly increased in the stimulated hNPC-containing CNGs compared to the unstimulated ones (Fig. 1d). However, not all genes varied with stimulation. The gene expression of HBEGF was unaltered under electrical stimulation.

3.2 Electrically-stimulated hNPC-containing CNGs improve behavioral recovery

Restoration of functional outcomes is the ultimate goal of PNI treatments. To test the restoration of motor and sensory recovery with electrically-stimulated stem cell therapy, we implanted CNGs with or without electrical stimulation, and hNPC-containing CNGs with or without electrical stimulation (Fig. 2a–c). Prior to implantation, all animals received behavioral training. Subsequently, CNGs were implanted into animals with a sciatic nerve transection surgery. Electrical stimulation based on the same *in vitro* stimulating parameters (40 V/m at 100 Hz for 1 hour) was applied immediately on day 1, 3, and 5 followed by weekly behavior analysis (Fig. 2a–c). The one-hour electrical stimulation was used because our *in vitro* data showed significant upregulation of neurotrophic factor expression in the stimulated hNPCs-containing CNGs. Moreover, shorter stimulation (1 hour) has previously been shown to be more effective than long duration of stimulation (from 3 hour to 14 days) in promoting axonal regeneration[50].

Studies of peripheral axon regeneration indicated that the prognosis for functional recovery is poor when muscle re-innervation is delayed, resulting in a lower force production than normal[51–53]. We first evaluated the muscular strength of the injured legs compared to that of healthy contralateral sides in the animals based on the grip strength test. We determined that the stimulated hNPC-containing CNGs showed the highest muscular gripping force compared to all other groups at the end of 12 weeks (Fig. 3a). We further assessed motor recovery using positional placing response and extensor postural thrust, in which proprioception and amount of force production were quantified, respectively. In the positional placing response, unstimulated and stimulated hNPC-containing CNGs showed early improvement in proprioception starting at week 1 (Fig. 3b). Interestingly, the stimulated hNPC-containing CNGs demonstrated sustained significant improvement throughout the entirety of the study. Similarly, the stimulated hNPC-containing CNGs significantly outperformed all other groups in the amount of force being produced from the injured legs in the extensor postural thrust (week 12: $p \leq 0.0001$ for “CNGs+Cells+ES” vs “CNGs+Cells”, “CNGs+ES”, and “CNGs”) (Fig. 3c). We observed that sensory recovery from thermal nociception occurred as early as week 2 in stimulated hNPC-containing CNGs, but all experimental groups retained some levels of sensory function without discernible difference among them starting at week 3 (Supplementary Fig. 4). In summation, these behavior results suggest that electrical stimulation accelerates behavioral recovery in

combination with stem cell therapy via CNGs to improve functional outcomes associated with PNI.

To evaluate the end-organ effect of our treatment approach, we next examined muscular changes. Muscle atrophy is a common debilitating symptom associated with peripheral nerve injuries[7,51,52,54,55]. The gastrocnemius muscle, a muscle that is innervated by the tibial branch of the sciatic nerve[56], was analyzed. The stimulated hNPC-containing CNGs restored significantly more muscle mass than the other treatment and control groups (Fig. 4). The ability to reduce end organ atrophy contributes to effective functional recovery.

3.3 Electrically-stimulated hNPCs restore electrophysiology in regenerated nerves

Electrophysiology was utilized to further assess the functional recovery of the regenerated nerves and their affected muscles. The compound action potential was measured in response to the sciatic nerve stimulation-induced at the proximal nerve stump above the CNG and recorded on the outside paw of the treated leg at the end of 12 weeks[41,43](Fig. 5a). Compound action potentials were observed only from conditions in which hNPCs were incorporated in the CNGs, illustrating proper electrical function from the regenerated nerves in those groups (Fig. 5a). We suspect that the absence of the compound action potential from non-cells groups was due to insufficient quantities of regenerated nerve fibers and/or inadequate levels of myelination during the regeneration. Conduction velocity, a key marker to indicate the health of the peripheral nerve for diseases[42,57], was higher in the stimulated hNPC-containing CNGs than the unstimulated animals (Fig. 5b). The elicited amplitude was also higher in the stimulated hNPC-containing CNGs than other groups (Fig. 5b). These data demonstrate that the implanted hNPCs are critical in promoting functional nerve regeneration and that interactive effect of electrical therapy further improves the ability of regenerated nerves to transmit electrical signals.

3.4 Electrically-stimulated hNPCs support optimal nerve regeneration

To support our functional analysis of the regenerated nerves with anatomical data, histological evaluation was performed at the 12-week time point. Using H&E staining, we observed qualitatively that the proximal end of all nerve guides showed better-aligned nerves fibers than those observed in the distal end (Supplementary Fig. 5). Both unstimulated and stimulated hNPC-containing CNGs showed more aligned nerve fibers, but stimulated hNPC-containing CNGs presented well-organized myelin sheets and more round axons. Without hNPCs, CNGs alone did not show any regenerated fibers while electrical-stimulated CNGs exhibited disorganized nerve fibers and areas of edema. The morphology of nerve axons in the stimulated hNPC-containing CNGs closely resembled the compact and aligned structure of healthy nerves.

Distal nerve stumps are known to degenerate quickly (<1 month) without proper reinnervation, affecting the viability of motor and sensory target organs (e.g. muscles) [58,59]. Therefore, we analyzed distal regions of all transplanted constructs in more detail with toluidine blue staining. Microscopically, unstimulated and stimulated hNPC-containing CNGs showed more densely packed nerve fibers in the center and edge of the conduits (Fig. 6a). In contrast, few loose fibers were observed in the unstimulated and stimulated CNGs

(Fig. 6a). In the stimulated CNGs, there were more fibers exhibited on the edge whereas connective tissues presented in the center of the conduits. We found a significant increase in the amount of nerve fibers and increased myelination in the stimulated hNPC-containing CNGs compared to other conditions (Fig. 6b). Interestingly, the number of nerve fibers was similar between the stimulated hNPC-containing CNGs and healthy group, but the level of myelination in the stimulated hNPC-containing CNGs was not as high as in the healthy nerves (Fig. 6b).

To investigate if the myelination was adequate, we evaluated the g-ratio of the regenerative nerves. The g-ratio has been widely used to indicate the functional and structural properties of optimal axonal myelination[60,61]. It is defined as the ratio between the inner axonal diameter to the total outer diameter. We analyzed the relationship between myelination and axon diameter (Fig. 7a). It became apparent that stimulated hNPC-containing CNGs not only presented bigger diameter fibers, but also their large diameter fibers were adequately myelinated with a consistent g-ratio ~0.62. Healthy nerves showed that their g-ratios slightly decreased as the axon diameters increased substantially. The linear relationship between g-ratio and axonal diameter from the stimulated hNPC-containing CNGs was much closer to the healthy group than other conditions. Unstimulated hNPC-containing CNGs exhibited some big diameter fibers, but they were not well-myelinated as indicated by the increased slope (R square value) in g-ratio. Interestingly, the stimulated CNGs showed an even greater degree of inconsistency in g-ratio compared to the unstimulated CNGs as indicated by their R square values quantified for variability. There was significant difference between the R square values from the stimulated hNPC-containing CNGs and healthy groups compared to the stimulated CNGs. Based on the frequency histogram (Fig. 7b), we observed that stimulated hNPC-containing CNGs had most of the fibers fall within the g-ratio range ~0.61–0.65; for unstimulated hNPC-containing CNGs ~0.73–0.77; for unstimulated and stimulated CNGs ~0.69–0.73 and 0.65–0.69, respectively. The g-ratio range ~0.61–0.65 in the stimulated hNPC-containing CNGs was much closer to that of ~0.53–0.57 in the healthy group than any other conditions. The average g-ratio was 0.62±0.07 for the stimulated hNPC-containing CNGs, which was lower than the g-ratios of 0.72±0.02, 0.71±0.03, 0.70±0.04 for unstimulated CNGs, stimulated CNGs, and unstimulated hNPC-containing CNGs, respectively (Supplementary Fig. 6). That g-ratio value was also closer to the actual g-ratio of 0.55±0.02 from the healthy group calculated based on experimental data (Supplementary Fig. 6). The g-ratio value from the stimulated hNPC-containing CNGs matches well with the optimal g-ratio predicted based on the speed of nerve fiber conduction in peripheral fibers (≈0.6)[61]. These findings on nerve diameter and myelination are consistent with the functional electrophysiology (Fig. 5) and behavioral results (Fig. 3). The lack of electrophysiological response from unstimulated and stimulated CNGs was likely caused by the insufficient number of myelinated fibers in those conditions. The adequately myelinated nerve fibers produced better conduction velocity and higher amplitude as demonstrated in the stimulated hNPC-containing CNGs followed by unstimulated hNPC-containing CNGs. We conclude that stimulated hNPC-containing CNGs provide the optimal conditions for the regeneration and myelination of sizeable nerves.

We further evaluated expression levels of axon and Schwann cell biomarkers, neurofilament and S100, for the regenerated nerves. Both unstimulated and stimulated hNPC-containing

CNGs exhibited high expression of neurofilament and S100, which were significantly greater than unstimulated and stimulated CNGs (Fig. 8a,b). We assessed hNPC survival in the CNGs and found that hNPCs died within one week after implantation under both unstimulated and stimulation conditions (Supplementary Fig. 7). This suggests that the main mechanism of nerve regeneration with implanted hNPC-containing CNGs is unrelated to long-term hNPC survival, differentiation, and integration. We hypothesized that the discrepancy in cell-induced nerve regeneration might be due to a sustained effect of increased neurotrophic factor release from hNPCs during the process of nerve regeneration. To test this hypothesis, we analyzed the Trk receptors that are known to bind to neurotrophic factors with high affinity and specificity[37,38]. The expression of Trk receptors was significantly elevated in the stimulated hNPC-containing CNG animals compared to other groups (Fig. 9). This data suggests that electrical treatment further improves the production of neurotrophic factors from hNPCs to achieve nerve regeneration through Trk-mediated pathways.

4. Discussion

This is the first study to illustrate a combined therapeutic strategy with implantable conductive polymer nerve guides that allow the *in vivo* delivery of electrical stimulation on transplanted stem cells to accelerate peripheral nerve recovery in animals. Our results demonstrate that the combined effect of electrical stimulation and stem cells promotes nerve regeneration with improved functional outcomes. We first show that CNGs can deliver an electric field to significantly upregulate the gene expression of neurotrophic factors (e.g. BDNF, NTF-3) in hNPCs without affecting their survival (Fig. 1). The rationale behind evaluating expression of neurotrophic factors such as BDNF and NTF-3 was because these factors are known for improved functional recovery associated with angiogenesis, axon projection, dendrite pruning, synapse formation, and patterning of neuronal network and innervation[26–30]. Our previous work also demonstrated that electrical stimulation modulates neurotrophic factor expression using different stimulating platforms and human neural progenitor cells[31,34,39]. The expression of HBEGF was studied because electrical stimulation modulates signaling pathways (e.g. EGFR/MAPK pathway) involved with cell mobilization and survival[62,63]. HBEGF was the key in stimulating the formation of multipotent glial-derived progenitors in the uninjured Zebrafish retina linking its role in the mediation of the EGFR/MAPK signal transduction pathway[64]. We evaluated the HBEGF expression but found no change under the electrical parameters used in this study. Subsequently, in the sciatic nerve transection model, the electrically stimulated hNPC-containing CNGs accelerated early sensory and motor recovery beginning on week 1–2 (Fig. 3b,c; Supplementary Fig. 4). Animals regained their sensory ability earlier in the combined therapy group which then normalized, whereas improved motor recovery was sustained. The increased neurotrophic factors released from electrically-stimulated stem cells appears to be an important mechcanism with increased TrK receptors on regenerated nerves observed with our approach. Our results appear to support a faster functional recovery compared to prior studies, in which sensory and motor nerve regeneration occurred from 2–3 weeks after sciatic nerve crush[65] or femoral nerve cut and repair[66] under electrical stimulation (30 minute to 1 hour) at low frequency (20 Hz). Our data also suggests that stem cells alone

provide a certain amount of nerve regeneration as seen in prior studies[67–69]. Yet, the combined effect of electrical stimulation and hNPC therapy significantly enhances functional outcomes compared to either therapy in isolation.

Few animal studies have investigated the effectiveness of combined therapeutic strategies through a comprehensive functional and anatomical assessment in treating peripheral nerve injuries (Supplementary Table 1)[36,50,70–81]. Therapeutic strategies such as *in vivo* electrical stimulation, polypyrrole-based conductive materials, and transplanted progenitor cells have been only studied in isolation. For example, stainless steel wires are commonly used and solely designed to apply electrical stimulation at the desired location to promote proliferation and recruitment of host's progenitor cells for spinal[76,77] or sensory nerve[50] repair. Conductive nerve guides offer both structural support and the ability to transmit electrical signals to the regenerated axons. Polypyrrole-based conductive nerve guides without transplanted cells and electrical stimulation showed regenerated nerves, but lacked functional information in treating spinal cord and peripheral nerve injuries[36,73–75]. Other conductive nerve guides made of polypyrrole-coated poly(l-lactic acid-co-ε-caprolactone)[70] or lysine-doped polypyrrole[71] with applied electrical stimulation showed some level of nerve regeneration with limited or no peripheral functional outcomes reported in animals. Transplantation of individual cell types such as adipose-derived stem cells[78,82], neural stem cells[79], Schwann cells[81], nucleus pulposus progenitor cells[80] was found to only improve certain aspects of functional recovery (e.g. muscle atrophy, electrophysiology) related to spinal and peripheral injuries. Our CNGs described in this study meet the critical need of a new platform that enables researchers to investigate the therapeutic potential of combined regenerative approaches to treat peripheral nerve injuries.

Muscle atrophy is an important limiting factor for functional recovery after nerve injury[7,51,52,54,55]. The combined therapy such as those of voluntary exercise and human skeletal muscle-derived stem cell transplantation has shown better functional recovery associated with long nerve defects[83,84]. We found that the use of electrical stimulation combined with hNPCs restores muscle mass in our study. Muscle atrophy occurs after the distal stump becomes denervated, completely incapable of supporting innervation after 6 months[57]. Therefore, it is critical for axons to reach their target organs, like muscle, during this regeneration period (up to 6 months)[57,85]. We found that stimulated hNPC-containing CNGs showed the most muscular gripping force and restored a considerable gastrocnemius muscle mass (Fig. 3a and Fig. 4). Furthermore, our electrophysiology demonstrated the ability of regenerated nerves and innervated muscles in the hNPC-containing CNGs to transmit electrical signals at satisfactory conduction velocities 12 weeks after nerve transection (Fig. 5). In addition to the quantitative measurements of downstream muscle strength and mass mentioned above, future studies looking at muscle pathology (i.e. Masson's trichrome) and functions (i.e. contraction) would be ideal to evaluate the eventual muscle recovery. Given the data presented here, it is clear that the stimulated CNGs containing hNPCs result in a dramatic improvement of functional nerve recovery, followed by unstimulated CNGs containing hNPCs.

Upon a closer examination of the regenerated nerves at the distal ends of the CNGs, we found a higher number of axons accompanied by more adequate myelin thickness with

optimal g-ratio ~0.6 in the stimulated hNPC-containing CNGs (Fig. 6 and Fig. 7). hNPCs were critical in the regeneration of axons, but the combined effect of hNPCs and electrical stimulation improved g-ratio and myelination of regenerated fibers (Fig. 6 and Fig. 7). Previous studies evaluating electrical stimulation alone found low levels of electrical stimulation (10–20Hz) increased axon myelination *in vitro*[86] and injured facial nerve rats[87]. The higher expression levels of neurofilament and S100 correlated well with the regeneration outcome in the late stages of nerve repair[58] (Fig. 8). We hypothesized that the regenerated nerve fibers with increased myelination were induced by the electrical stimulation of hNPCs causing increased neurotrophic factor release. Normally, neurotrophic factors are expressed immediately after nerve injury and peak within 1 month[88,89]. However, during the prolonged denervation period (>1 month) of the distal nerve stump, the expression of the neurotrophic factors and their receptors is not sustained and declines with time[58,59]. Previous work demonstrated that elevated BDNF in the chronically axotomized neurons was observed after 21 days post-repair under electrical stimulation (20 Hz for 1 hour)[88]. In our results, the expression of Trk receptors that bind with neurotrophic factors was expressed at a high level, indicating successful nerve regeneration at the distal end from the stimulated hNPC-containing CNGs even after 12 weeks (Fig. 9).

Electrical stimulation alone in the first week after injury, as demonstrated by the stimulated CNGs group, was not sufficient to promote nerve regeneration and functional recovery. The stimulated CNGs group displayed a limited number of regenerated fibers (Fig. 6), which was not significant to improve functional recovery and reinnervate with their affected muscles (Fig. 3,4,5). Only in the presence of transplanted hNPCs, there was significant improvement with additive benefits from electrical stimulation for accelerated recovery. This was possibly due to that electrical stimulation parameters were optimized specifically to enhance the therapeutic potential of transplanted hNPCs. Our data suggests the main mechanism for hNPCs to promote recovery is through changes associated with neurotrophic factors and their Trk-binding receptors in the CNGs under electrical stimulation. In our study, the hNPC died quickly in CNGs after 7 days of implantation. These results suggest any small number of surviving hNPCs is likely not sufficient to explain the observed structural and functional recovery (Supplementary Fig. 7). The exact cellular mechanisms that transduce electrical signals into cellular changes remain unknown. The mechanisms that resulted in gene changes could be influenced by direct electrical field effects as well as metabolic activity changes. Our previous study indicated that hNPC properties, including change in neurotrophic factor expression, can be manipulated depending on the physical nature of electrical stimulating platforms as well as their cellular metabolic states[39]. The next steps of elucidating Trk-related mechanistic pathways are needed to understand how electrical signals are transduced into cellular activities that promote peripheral recovery.

It is worth noting that the choice of the stem cell source can be critical in designing an effective stem cell-containing conductive nerve guides combined with electrical stimulation. Stem cell sources that originate from the neural crest, such as human dental pulp stem cells[90,91] or dental mesenchymal stem cells[92,93], could potentially ensure a prolonged cell survival and present an even stronger regenerative effect from sustained release of neurotrophic factors to treat peripheral nerve injuries. For instance, the sustained expression of neurotrophic factor BDNF was observed in the vicinity of the transplanted dental human

mesenchymal stem cells for 2 weeks to promote axonal regeneration in rats with sciatic nerve injury[93]. These types of adult stem cells are easily accessible and capable of rapid expansion and share similar molecular and phenotypic properties to Schwann cells, making them an effective alternative for the cell treatment of nerve injuries. It would be necessary to explore the optimal stem cell source combined with our electrically-stimulated conductive nerve guides to develop better regenerative strategies in the future.

Our findings represent an important step in the regenerative rehabilitation approach by using electrical stimulation to enhance the therapeutic potential of stem cell-based treatments for peripheral nerve injuries. Overall, we demonstrate significant improvement in peripheral nerve repair through a new platform for combined electrical stimulation and stem cell delivery. Other types of peripheral nerve injuries in locations such as arms and hands could also readily benefit from the treatment strategies presented here. Biodegradable conductive nerve guides (e.g. composites made of PPy and other materials such as polyvinyl alcohol (PVA)[100], poly(L-lactide) (PLLA)[101] or poly(ε-caprolactone) (PCL)[101,102]) that allow controlled material degradation and eliminates the need of nerve guide removal could be further explored in our regenerative strategy. New strategies based on manipulating the physiological stem cell microenvironment to introduce physical, chemical, and electrical stimuli may amplify stem cell effects on neural recovery, thus increasing their therapeutic efficacy.

Supplementary Material

Refer to Web version on PubMed Central for supplementary material.

Acknowledgements:

We would like to thank Pauline Chu for her advice on tissue processing and Patrick Paine on demonstrating how to use the gripper. We would like to thank Byeongtaek Oh for his advice on stem cell protocols and conductive polymer stimulation. This research was supported by the Stanford University Dean's Postdoctoral Fellowship and the Eunice Kennedy Shriver National Institute of Child Health & Human Development (NICHD) of the National Institutes of Health (NIH) under Award Number F32HD098808 (SS), the Alliance for Regenerative Rehabilitation Research and Training (P2C HD08684) and NIH K08NS089976 (PMG).

Reference

[1]. Foster CH, Karsy M, Jensen MR, Guan J, Eli I, Mahan MA, Trends and Cost-Analysis of Lower Extremity Nerve Injury Using the National Inpatient Sample, Neurosurgery. 85 (2019) 250–256. 10.1093/neuros/nyy265. [PubMed: 29889258]

[2]. Karsy M, Watkins R, Jensen MR, Guan J, Brock AA, Mahan MA, Trends and Cost Analysis of Upper Extremity Nerve Injury Using the National (Nationwide) Inpatient Sample, World Neurosurg. 123 (2019) e488–e500. 10.1016/j.wneu.2018.11.192. [PubMed: 30502477]

[3]. Sunderland S, Rate of regeneration in human peripheral nerves; analysis of the interval between injury and onset of recovery, Arch Neurol Psychiatry. 58 (1947) 251–295.

[4]. Black MM, Lasek RJ, Slowing of the rate of axonal regeneration during growth and maturation, Exp. Neurol 63 (1979) 108–119. [PubMed: 467539]

[5]. Nath RK, Melcher SE, Rapid recovery of serratus anterior muscle function after microneurolysis of long thoracic nerve injury, J Brachial Plex Peripher Nerve Inj. 2 (2007) 4. 10.1186/1749-7221-2-4. [PubMed: 17291339]

[6]. Campbell WW, Evaluation and management of peripheral nerve injury, Clin Neurophysiol. 119 (2008) 1951–1965. 10.1016/j.clinph.2008.03.018. [PubMed: 18482862]

[7]. Kaplan HM, Mishra P, Kohn J, The overwhelming use of rat models in nerve regeneration research may compromise designs of nerve guidance conduits for humans, J Mater Sci Mater Med. 26 (2015). 10.1007/s10856-015-5558-4.

[8]. di Summa PG, Kalbermatten DF, Pralong E, Raffoul W, Kingham PJ, Terenghi G, Long-term in vivo regeneration of peripheral nerves through bioengineered nerve grafts, Neuroscience. 181 (2011) 278–291. 10.1016/j.neuroscience.2011.02.052. [PubMed: 21371534]

[9]. Pereira Lopes FR, Camargo de Moura Campos L. , Dias Corrêa J, Balduino A, Lora S, Langone F, Borojevic R, Blanco Martinez AM, Bone marrow stromal cells and resorbable collagen guidance tubes enhance sciatic nerve regeneration in mice, Exp. Neurol 198 (2006) 457–468. 10.1016/j.expneurol.2005.12.019. [PubMed: 16487971]

[10]. Jenkins PM, Laughter MR, Lee DJ, Lee YM, Freed CR, Park D, A nerve guidance conduit with topographical and biochemical cues: potential application using human neural stem cells, Nanoscale Res Lett. 10 (2015). 10.1186/s11671-015-0972-6.

[11]. Ni H-C, Tseng T-C, Chen J-R, Hsu S-H, Chiu I-M, Fabrication of bioactive conduits containing the fibroblast growth factor 1 and neural stem cells for peripheral nerve regeneration across a 15 mm critical gap, Biofabrication. 5 (2013) 035010. 10.1088/1758-5082/5/3/035010.

[12]. Salomone R, Bento RF, Costa HJZR, Azzi-Nogueira D, Ovando PC, Da-Silva CF, Zanatta DB, Strauss BE, Haddad LA, Bone marrow stem cells in facial nerve regeneration from isolated stumps, Muscle Nerve. 48 (2013) 423–429. 10.1002/mus.23768. [PubMed: 23824709]

[13]. Carrier-Ruiz A, Evaristo-Mendonça F, Mendez-Otero R, Ribeiro-Resende VT, Biological behavior of mesenchymal stem cells on poly-ε-caprolactone filaments and a strategy for tissue engineering of segments of the peripheral nerves, Stem Cell Research & Therapy. 6 (2015) 128. 10.1186/s13287-015-0121-2. [PubMed: 26149068]

[14]. Pang C-J, Tong L, Ji L-L, Wang Z-Y, Zhang X, Gao H, Jia H, Zhang L-X, Tong X-J, Synergistic effects of ultrashort wave and bone marrow stromal cells on nerve regeneration with acellular nerve allografts, Synapse. 67 (2013) 637–647. 10.1002/syn.21669. [PubMed: 23554017]

[15]. Weightman A, Jenkins S, Pickard M, Chari D, Yang Y, Alignment of multiple glial cell populations in 3D nanofiber scaffolds: toward the development of multicellular implantable scaffolds for repair of neural injury, Nanomedicine. 10 (2014) 291–295. 10.1016/j.nano.2013.09.001. [PubMed: 24090767]

[16]. Tse C, Whiteley R, Yu T, Stringer J, MacNeil S, Haycock JW, Smith PJ, Inkjet printing Schwann cells and neuronal analogue NG108–15 cells, Biofabrication. 8 (2016) 015017. 10.1088/1758-5090/8/1/015017.

[17]. Hu Y, Wu Y, Gou Z, Tao J, Zhang J, Liu Q, Kang T, Jiang S, Huang S, He J, Chen S, Du Y, Gou M, 3D-engineering of Cellularized Conduits for Peripheral Nerve Regeneration, Sci Rep. 6 (2016) 32184. 10.1038/srep32184.

[18]. Akhavan O, Ghaderi E, Shirazian SA, Rahighi R, Rolled graphene oxide foams as three-dimensional scaffolds for growth of neural fibers using electrical stimulation of stem cells, Carbon. 97 (2016) 71–77. 10.1016/j.carbon.2015.06.079.

[19]. Li N, Zhang X, Song Q, Su R, Zhang Q, Kong T, Liu L, Jin G, Tang M, Cheng G, The promotion of neurite sprouting and outgrowth of mouse hippocampal cells in culture by graphene substrates, Biomaterials. 32 (2011) 9374–9382. 10.1016/j.biomaterials.2011.08.065. [PubMed: 21903256]

[20]. Lladó J, Haenggeli C, Maragakis NJ, Snyder EY, Rothstein JD, Neural stem cells protect against glutamate-induced excitotoxicity and promote survival of injured motor neurons through the secretion of neurotrophic factors, Mol. Cell. Neurosci 27 (2004) 322–331. 10.1016/j.mcn.2004.07.010. [PubMed: 15519246]

[21]. Xu L, Zhou S, Feng G-Y, Zhang L-P, Zhao D-M, Sun Y, Liu Q, Huang F, Neural stem cells enhance nerve regeneration after sciatic nerve injury in rats, Mol. Neurobiol 46 (2012) 265–274. 10.1007/s12035-012-8292-7. [PubMed: 22806359]

[22]. Huang EJ, Reichardt LF, Trk receptors: roles in neuronal signal transduction, Annu Rev Biochem. 72 (2003) 609–642. 10.1146/annurev.biochem.72.121801.161629. [PubMed: 12676795]

[23]. Reichardt LF, Neurotrophin-regulated signalling pathways, Philos Trans R Soc Lond B Biol Sci. 361 (2006) 1545–1564. 10.1098/rstb.2006.1894. [PubMed: 16939974]

[24]. Asano Y, Nagasaki A, Uyeda TQP, Correlated waves of actin filaments and PIP3 in Dictyostelium cells, Cell Motil Cytoskeleton. 65 (2008) 923–934. 10.1002/cm.20314. [PubMed: 18814278]

[25]. Inagaki N, Katsuno H, Actin Waves: Origin of Cell Polarization and Migration?, Trends Cell Biol. 27 (2017) 515–526. 10.1016/j.tcb.2017.02.003. [PubMed: 28283221]

[26]. Huang EJ, Reichardt LF, Neurotrophins: roles in neuronal development and function, Annu. Rev. Neurosci 24 (2001) 677–736. 10.1146/annurev.neuro.24.1.677. [PubMed: 11520916]

[27]. Chalazonitis A, Pham TD, Rothman TP, DiStefano PS, Bothwell M, Blair-Flynn J, Tessarollo L, Gershon MD, Neurotrophin-3 is required for the survival-differentiation of subsets of developing enteric neurons, J. Neurosci 21 (2001) 5620–5636. [PubMed: 11466433]

[28]. Henderson CE, Role of neurotrophic factors in neuronal development, Curr. Opin. Neurobiol 6 (1996) 64–70. [PubMed: 8794045]

[29]. Cohen-Cory S, Fraser SE, Effects of brain-derived neurotrophic factor on optic axon branching and remodelling in vivo, Nature. 378 (1995) 192–196. 10.1038/378192a0. [PubMed: 7477323]

[30]. Sebert ME, Shooter EM, Expression of mRNA for neurotrophic factors and their receptors in the rat dorsal root ganglion and sciatic nerve following nerve injury, J. Neurosci. Res 36 (1993) 357–367. 10.1002/jnr.490360402. [PubMed: 8271314]

[31]. Song S, George PM, Conductive polymer scaffolds to improve neural recovery, Neural Regen Res. 12 (2017) 1976–1978. 10.4103/1673-5374.221151. [PubMed: 29323032]

[32]. George PM, Bliss TM, Hua T, Lee A, Oh B, Levinson A, Mehta S, Sun G, Steinberg GK, Electrical preconditioning of stem cells with a conductive polymer scaffold enhances stroke recovery, Biomaterials. 142 (2017) 31–40. 10.1016/j.biomaterials.2017.07.020. [PubMed: 28719819]

[33]. George PM, Lyckman AW, LaVan DA, Hegde A, Leung Y, Avasare R, Testa C, Alexander PM, Langer R, Sur M, Fabrication and biocompatibility of polypyrrole implants suitable for neural prosthetics, Biomaterials. 26 (2005) 3511–3519. 10.1016/j.biomaterials.2004.09.037. [PubMed: 15621241]

[34]. Oh B, Levinson A, Lam V, Song S, George P, Electrically Conductive Scaffold to Modulate and Deliver Stem Cells, J Vis Exp. (2018). 10.3791/57367.

[35]. Stewart E, Kobayashi NR, Higgins MJ, Quigley AF, Jamali S, Moulton SE, Kapsa RMI, Wallace GG, Crook JM, Electrical stimulation using conductive polymer polypyrrole promotes differentiation of human neural stem cells: a biocompatible platform for translational neural tissue engineering, Tissue Eng Part C Methods. 21 (2015) 385–393. 10.1089/ten.TEC.2014.0338. [PubMed: 25296166]

[36]. George PM, Saigal R, Lawlor MW, Moore MJ, LaVan DA, Marini RP, Selig M, Makhni M, Burdick JA, Langer R, Kohane DS, Three-dimensional conductive constructs for nerve regeneration, Journal of Biomedical Materials Research Part A. 91A (2009) 519–527. 10.1002/jbm.a.32226.

[37]. Barbacid M, The Trk family of neurotrophin receptors, J. Neurobiol 25 (1994) 1386–1403. 10.1002/neu.480251107. [PubMed: 7852993]

[38]. Chao MV, Neurotrophins and their receptors: a convergence point for many signalling pathways, Nat. Rev. Neurosci 4 (2003) 299–309. 10.1038/nrn1078. [PubMed: 12671646]

[39]. Song S, Amores D, Chen C, McConnell K, Oh B, Poon A, George PM, Controlling properties of human neural progenitor cells using 2D and 3D conductive polymer scaffolds, Sci Rep. 9 (2019) 19565. 10.1038/s41598-019-56021-w.

[40]. Kohane DS, Yieh J, Lu NT, Langer R, Strichartz GR, Berde CB, A re-examination of tetrodotoxin for prolonged duration local anesthesia, Anesthesiology. 89 (1998) 119–131. [PubMed: 9667302]

[41]. Mokarram N, Dymanus K, Srinivasan A, Lyon JG, Tipton J, Chu J, English AW, Bellamkonda RV, Immunoengineering nerve repair, Proc. Natl. Acad. Sci. U.S.A 114 (2017) E5077–E5084. 10.1073/pnas.1705757114.

[42]. Liu Y, Li J, Song S, Kang J, Tsao Y, Chen S, Mottni V, McConnell K, Xu W, Zheng Y-Q, Tok JB-H, George PM, Bao Z, Morphing electronics enable neuromodulation in growing tissue, Nat. Biotechnol (2020). 10.1038/s41587-020-0495-2.

[43]. Hort-Legrand C, Noah L, Mériguet E, Mésangeau D, Motor and sensory nerve conduction velocities in Yucatan minipigs, Lab. Anim 40 (2006) 53–57. 10.1258/002367706775404345. [PubMed: 16460588]

[44]. Franchi S, Valsecchi AE, Borsani E, Procacci P, Ferrari D, Zalfa C, Zaffa C, Sartori P, Rodella LF, Vescovi A, Maione S, Rossi F, Sacerdote P, Colleoni M, Panerai AE, Intravenous neural stem cells abolish nociceptive hypersensitivity and trigger nerve regeneration in experimental neuropathy, Pain. 153 (2012) 850–861. 10.1016/j.pain.2012.01.008. [PubMed: 22321918]

[45]. Guo B-F, Dong M-M, Application of neural stem cells in tissue-engineered artificial nerve, Otolaryngol Head Neck Surg. 140 (2009) 159–164. 10.1016/j.otohns.2008.10.039. [PubMed: 19201281]

[46]. Zhao M, Bai H, Wang E, Forrester JV, McCaig CD, Electrical stimulation directly induces pre-angiogenic responses in vascular endothelial cells by signaling through VEGF receptors, J. Cell. Sci 117 (2004) 397–405. 10.1242/jcs.00868. [PubMed: 14679307]

[47]. Amaral SL, Linderman JR, Morse MM, Greene AS, Angiogenesis induced by electrical stimulation is mediated by angiotensin II and VEGF, Microcirculation. 8 (2001) 57–67. [PubMed: 11296854]

[48]. Huang J, Hu X, Lu L, Ye Z, Zhang Q, Luo Z, Electrical regulation of Schwann cells using conductive polypyrrole/chitosan polymers, J Biomed Mater Res A. 93 (2010) 164–174. 10.1002/jbm.a.32511. [PubMed: 19536828]

[49]. Xiang Y, Liu H, Yan T, Zhuang Z, Jin D, Peng Y, Functional electrical stimulation-facilitated proliferation and regeneration of neural precursor cells in the brains of rats with cerebral infarction, Neural Regen Res. 9 (2014) 243–251. 10.4103/1673-5374.128215. [PubMed: 25206808]

[50]. Geremia NM, Gordon T, Brushart TM, Al-Majed AA, Verge VMK, Electrical stimulation promotes sensory neuron regeneration and growth-associated gene expression, Exp. Neurol 205 (2007) 347–359. 10.1016/j.expneurol.2007.01.040. [PubMed: 17428474]

[51]. Finkelstein DI, Dooley PC, Luff AR, Recovery of muscle after different periods of denervation and treatments, Muscle Nerve. 16 (1993) 769–777. 10.1002/mus.880160712. [PubMed: 8505933]

[52]. Fu SY, Gordon T, Contributing factors to poor functional recovery after delayed nerve repair: prolonged denervation, J. Neurosci 15 (1995) 3886–3895. [PubMed: 7751953]

[53]. Grumbles RM, Sesodia S, Wood PM, Thomas CK, Neurotrophic factors improve motoneuron survival and function of muscle reinnervated by embryonic neurons, J. Neuropathol. Exp. Neurol 68 (2009) 736–746. 10.1097/NEN.0b013e3181a9360f. [PubMed: 19535998]

[54]. Bennett GJ, Xie YK, A peripheral mononeuropathy in rat that produces disorders of pain sensation like those seen in man, Pain. 33 (1988) 87–107. [PubMed: 2837713]

[55]. M F G, Khan MM,HS,WS, Peripheral nerve injury: principles for repair and regeneration, Open Orthop J. 8 (2014) 199–203. 10.2174/1874325001408010199. [PubMed: 25067975]

[56]. Sarabia-Estrada R, Bañuelos-Pineda J, Osuna Carrasco LP, Jiménez-Vallejo S, Jiménez-Estrada I, Rivas-Celis E, Dueñas-Jiménez JM, Dueñas-Jiménez SH, Aberrant gastrocnemius muscle innervation by tibial nerve afferents after implantation of chitosan tubes impregnated with progesterone favored locomotion recovery in rats with transected sciatic nerve, J. Neurosurg 123 (2015) 270–282. 10.3171/2014.12.JNS132519. [PubMed: 25679274]

[57]. Scheib J, Höke A, Advances in peripheral nerve regeneration, Nat Rev Neurol. 9 (2013) 668–676. 10.1038/nrneurol.2013.227. [PubMed: 24217518]

[58]. Boyd JG, Gordon T, Neurotrophic factors and their receptors in axonal regeneration and functional recovery after peripheral nerve injury, Mol. Neurobiol 27 (2003) 277–324. 10.1385/MN:27:3:277. [PubMed: 12845152]

[59]. Höke A, Redett R, Hameed H, Jari R, Zhou C, Li ZB, Griffin JW, Brushart TM, Schwann cells express motor and sensory phenotypes that regulate axon regeneration, J. Neurosci 26 (2006) 9646–9655. 10.1523/JNEUROSCI.1620-06.2006. [PubMed: 16988035]

[60]. Chomiak T, Hu B, What Is the Optimal Value of the g-Ratio for Myelinated Fibers in the Rat CNS? A Theoretical Approach, PLoS One. 4 (2009). 10.1371/journal.pone.0007754.

[61]. Rushton W. a. H., A theory of the effects of fibre size in medullated nerve, J. Physiol. (Lond.) 115 (1951) 101–122. 10.1113/jphysiol.1951.sp004655. [PubMed: 14889433]

[62]. Rosen LB, Greenberg ME, Stimulation of growth factor receptor signal transduction by activation of voltage-sensitive calcium channels., Proc Natl Acad Sci U S A. 93 (1996) 1113–1118. [PubMed: 8577724]

[63]. Tsai H-F, Huang C-W, Chang H-F, Chen JJW, Lee C-H, Cheng J-Y, Evaluation of EGFR and RTK Signaling in the Electrotaxis of Lung Adenocarcinoma Cells under Direct-Current Electric Field Stimulation, PLOS ONE. 8 (2013) e73418. 10.1371/journal.pone.0073418.

[64]. Wan J, Ramachandran R, Goldman D, HB-EGF is necessary and sufficient for Müller glia dedifferentiation and retina regeneration, Dev Cell. 22 (2012) 334–347. 10.1016/j.devcel.2011.11.020. [PubMed: 22340497]

[65]. Alrashdan MS, Park J-C, Sung M-A, Yoo SB, Jahng JW, Lee TH, Kim S-J, Lee J-H, Thirty minutes of low intensity electrical stimulation promotes nerve regeneration after sciatic nerve crush injury in a rat model, Acta Neurol Belg. 110 (2010) 168–179. [PubMed: 20873447]

[66]. Al-Majed AA, Neumann CM, Brushart TM, Gordon T, Brief electrical stimulation promotes the speed and accuracy of motor axonal regeneration, J. Neurosci 20 (2000) 2602–2608. [PubMed: 10729340]

[67]. Cheng L-N, Duan X-H, Zhong X-M, Guo R-M, Zhang F, Zhou C-P, Shen J, Transplanted Neural Stem Cells Promote Nerve Regeneration in Acute Peripheral Nerve Traction Injury: Assessment Using MRI, American Journal of Roentgenology. 196 (2011) 1381–1387. 10.2214/AJR.10.5495. [PubMed: 21606303]

[68]. Wang C, Lu C, Peng J, Hu C, Wang Y, Roles of neural stem cells in the repair of peripheral nerve injury, Neural Regeneration Research. 12 (2017) 2106. 10.4103/1673-5374.221171. [PubMed: 29323053]

[69]. Dong M, Yi T, Stem Cell and Peripheral Nerve Injury and Repair, Facial Plast Surg. 26 (2010) 421–428. 10.1055/s-0030-1265023. [PubMed: 20853234]

[70]. Song J, Sun B, Liu S, Chen W, Zhang Y, Wang C, Mo X, Che J, Ouyang Y, Yuan W, Fan C, Polymerizing Pyrrole Coated Poly (l-lactic acid-co-ε-caprolactone) (PLCL) Conductive Nanofibrous Conduit Combined with Electric Stimulation for Long-Range Peripheral Nerve Regeneration, Front Mol Neurosci. 9 (2016) 117. 10.3389/fnmol.2016.00117. [PubMed: 27877111]

[71]. Zhang H, Wang K, Xing Y, Yu Q, Lysine-doped polypyrrole/spider silk protein/poly(l-lactic) acid containing nerve growth factor composite fibers for neural application, Mater Sci Eng C Mater Biol Appl. 56 (2015) 564–573. 10.1016/j.msec.2015.06.024. [PubMed: 26249628]

[72]. Raynald B. Shu X-B. Liu J-F Zhou H. Huang J-Y Wang X-D Sun C. Qin Y-H An, Polypyrrole/polylactic acid nanofibrous scaffold cotransplanted with bone marrow stromal cells promotes the functional recovery of spinal cord injury in rats, CNS Neuroscience & Therapeutics. 25 (2019) 951–964. 10.1111/cns.13135. [PubMed: 31486601]

[73]. Zhou L, Fan L, Yi X, Zhou Z, Liu C, Fu R, Dai C, Wang Z, Chen X, Yu P, Chen D, Tan G, Wang Q, Ning C, Soft Conducting Polymer Hydrogels Cross-Linked and Doped by Tannic Acid for Spinal Cord Injury Repair, ACS Nano. 12 (2018) 10957–10967. 10.1021/acsnano.8b04609.

[74]. Durgam H, Sapp S, Deister C, Khaing Z, Chang E, Luebben S, Schmidt CE, Novel degradable co-polymers of polypyrrole support cell proliferation and enhance neurite outgrowth with electrical stimulation, J Biomater Sci Polym Ed. 21 (2010) 1265–1282. 10.1163/092050609X12481751806330. [PubMed: 20534184]

[75]. Zhang Z, Rouabhia M, Wang Z, Roberge C, Shi G, Roche P, Li J, Dao LH, Electrically conductive biodegradable polymer composite for nerve regeneration: electricity-stimulated neurite outgrowth and axon regeneration, Artif Organs. 31 (2007) 13–22. 10.1111/j.1525-1594.2007.00335.x. [PubMed: 17209956]

[76]. Becker D, Gary DS, Rosenzweig ES, Grill WM, McDonald JW, Functional electrical stimulation helps replenish progenitor cells in the injured spinal cord of adult rats, Exp. Neurol 222 (2010) 211–218. 10.1016/j.expneurol.2009.12.029. [PubMed: 20059998]

[77]. Carmel JB, Berrol LJ, Brus-Ramer M, Martin JH, Chronic electrical stimulation of the intact corticospinal system after unilateral injury restores skilled locomotor control and promotes spinal axon outgrowth, J. Neurosci 30 (2010) 10918–10926. 10.1523/JNEUROSCI.1435-10.2010.

[78]. Saller MM, Huettl R-E, Mayer JM, Feuchtinger A, Krug C, Holzbach T, Volkmer E, Validation of a novel animal model for sciatic nerve repair with an adipose-derived stem cell loaded fibrin conduit, Neural Regen Res. 13 (2018) 854–861. 10.4103/1673-5374.232481. [PubMed: 29863016]

[79]. Poplawski GHD, Lie R, Hunt M, Kumamaru H, Kawaguchi R, Lu P, Schäfer MKE, Woodruff G, Robinson J, Canete P, Dulin JN, Geoffroy CG, Menzel L, Zheng B, Coppola G, Tuszynski MH, Adult rat myelin enhances axonal outgrowth from neural stem cells, Sci Transl Med. 10 (2018). 10.1126/scitranslmed.aal2563.

[80]. Ishii T, Sakai D, Schol J, Nakai T, Suyama K, Watanabe M, Sciatic nerve regeneration by transplantation of in vitro differentiated nucleus pulposus progenitor cells, Regen Med. 12 (2017) 365–376. 10.2217/rme-2016-0168. [PubMed: 28621199]

[81]. Yu K, Kocsis JD, Schwann cell engraftment into injured peripheral nerve prevents changes in action potential properties, J. Neurophysiol 94 (2005) 1519–1527. 10.1152/jn.00107.2005. [PubMed: 16061494]

[82]. Schilling BK, Schusterman MA, Kim D-Y, Repko AJ, Klett KC, Christ GJ, Marra KG, Adipose-derived stem cells delay muscle atrophy after peripheral nerve injury in the rodent model, Muscle Nerve. 59 (2019) 603–610. 10.1002/mus.26432. [PubMed: 30681163]

[83]. Tamaki T, Hirata M, Nakajima N, Saito K, Hashimoto H, Soeda S, Uchiyama Y, Watanabe M, A Long-Gap Peripheral Nerve Injury Therapy Using Human Skeletal Muscle-Derived Stem Cells (Sk-SCs): An Achievement of Significant Morphological, Numerical and Functional Recovery, PLOS ONE. 11 (2016) e0166639. 10.1371/journal.pone.0166639.

[84]. Seta H, Maki D, Kazuno A, Yamato I, Nakajima N, Soeda S, Uchiyama Y, Tamaki T, Voluntary Exercise Positively Affects the Recovery of Long-Nerve Gap Injury Following Tube-Bridging with Human Skeletal Muscle-Derived Stem Cell Transplantation, Journal of Clinical Medicine. 7 (2018) 67. 10.3390/jcm7040067.

[85]. Ma CHE, Omura T, Cobos EJ, Latrémolière A, Ghasemlou N, Brenner GJ, van Veen E, Barrett L, Sawada T, Gao F, Coppola G, Gertler F, Costigan M, Geschwind D, Woolf CJ, Accelerating axonal growth promotes motor recovery after peripheral nerve injury in mice, J. Clin. Invest 121 (2011) 4332–4347. 10.1172/JCI58675. [PubMed: 21965333]

[86]. Yang IH, Gary D, Malone M, Dria S, Houdayer T, Belegu V, McDonald JW, Thakor N, Axon myelination and electrical stimulation in a microfluidic, compartmentalized cell culture platform, Neuromolecular Med. 14 (2012) 112–118. 10.1007/s12017-012-8170-5. [PubMed: 22527791]

[87]. Deng Y, Xu Y, Liu H, Peng H, Tao Q, Liu H, Liu H, Wu J, Chen X, Fan J, Electrical stimulation promotes regeneration and re-myelination of axons of injured facial nerve in rats, Neurol. Res 40 (2018) 231–238. 10.1080/01616412.2018.1428390. [PubMed: 29513163]

[88]. Al-Majed AA, Tam SL, Gordon T, Electrical stimulation accelerates and enhances expression of regeneration-associated genes in regenerating rat femoral motoneurons, Cell. Mol. Neurobiol 24 (2004) 379–402. [PubMed: 15206821]

[89]. Al Majed AA, Brushart TM, Gordon T, Electrical stimulation accelerates and increases expression of BDNF and trkB mRNA in regenerating rat femoral motoneurons, European Journal of Neuroscience. 12 (2000) 4381–4390. 10.1111/j.1460-9568.2000.01341.x.

[90]. Sanen K, Martens W, Georgiou M, Ameloot M, Lambrichts I, Phillips J, Engineered neural tissue with Schwann cell differentiated human dental pulp stem cells: potential for peripheral nerve repair?, Journal of Tissue Engineering and Regenerative Medicine. 11 (2017) 3362–3372. 10.1002/term.2249. [PubMed: 28052540]

[91]. Carnevale G, Pisciotta A, Riccio M, Bertoni L, De Biasi S, Gibellini L, Zordani A, Cavallini GM, La Sala GB, Bruzzesi G, Ferrari A, Cossarizza A, de Pol A, Human dental pulp stem cells expressing STRO-1, c-kit and CD34 markers in peripheral nerve regeneration, J Tissue Eng Regen Med. 12 (2018) e774–e785. 10.1002/term.2378. [PubMed: 27943583]

[92]. Saito MT, Silvério KG, Casati MZ, Sallum EA, Nociti FH Jr, Tooth-derived stem cells: Update and perspectives, World J Stem Cells. 7 (2015) 399–407. 10.4252/wjsc.v7.i2.399. [PubMed: 25815123]

[93]. Kolar MK, Itte VN, Kingham PJ, Novikov LN, Wiberg M, Kelk P, The neurotrophic effects of different human dental mesenchymal stem cells, Scientific Reports. 7 (2017) 12605. 10.1038/s41598-017-12969-1.

[94]. Beltran MJ, Burns TC, Eckel TT, Potter BK, Wenke JC, Hsu JR, Skeletal Trauma Research Consortium (STReC), Fate of combat nerve injury, J Orthop Trauma. 26 (2012) e198–203. 10.1097/BOT.0b013e31823f000e. [PubMed: 22437422]

[95]. Dyck PJ, Lais AC, Giannini C, Engelstad JK, Structural alterations of nerve during cuff compression, PNAS. 87 (1990) 9828–9832. 10.1073/pnas.87.24.9828. [PubMed: 2263633]

[96]. Flores LP, Carneiro JZ, Peripheral nerve compression secondary to adjacent lipomas, Surg Neurol. 67 (2007) 258–262; discussion 262–263. 10.1016/j.surneu.2006.06.052. [PubMed: 17320633]

[97]. Huckhagel T, Nüchtern J, Regelsberger J, Lefering R, Nerve injury in severe trauma with upper extremity involvement: evaluation of 49,382 patients from the TraumaRegister DGU® between 2002 and 2015, Scand J Trauma Resusc Emerg Med. 26 (2018). 10.1186/s13049-018-0546-6.

[98]. Schlosshauer B, Dreesmann L, Schaller H-E, Sinis N, Synthetic nerve guide implants in humans: a comprehensive survey, Neurosurgery. 59 (2006) 740–747; discussion 747–748. 10.1227/01.NEU.0000235197.36789.42. [PubMed: 17038939]

[99]. Prasad M, Babiker M, Rao G, Rittey C, Pediatric sciatic neuropathy presenting as painful leg: A case report and review of literature, J Pediatr Neurosci. 8 (2013) 161–164. 10.4103/1817-1745.117858. [PubMed: 24082941]

[100]. Ribeiro J, Pereira T, Caseiro AR, Armada-da-Silva P, Pires I, Prada J, Amorim I, Amado S, França M, Gonçalves C, Lopes MA, Santos JD, Silva DM, Geuna S, Luís AL, Maurício AC, Evaluation of biodegradable electric conductive tube-guides and mesenchymal stem cells, World J Stem Cells. 7 (2015) 956–975. 10.4252/wjsc.v7.i6.956. [PubMed: 26240682]

[101]. Boutry CM, Gerber-Hörler I, Hierold C, Electrically conducting biodegradable polymer composites (polylactide-polypyrrole and polycaprolactone-polypyrrole) for passive resonant circuits, Polymer Engineering & Science. 53 (2013) 1196–1208. 10.1002/pen.23373.

[102]. Nguyen HT, Wei C, Chow JK, Nguyen A, Coursen J, Sapp S, Luebben S, Chang E, Ross R, Schmidt CE, Electric field stimulation through a biodegradable polypyrrole-co-polycaprolactone substrate enhances neural cell growth, J Biomed Mater Res A. 102 (2014) 2554–2564. 10.1002/jbm.a.34925. [PubMed: 23964001]

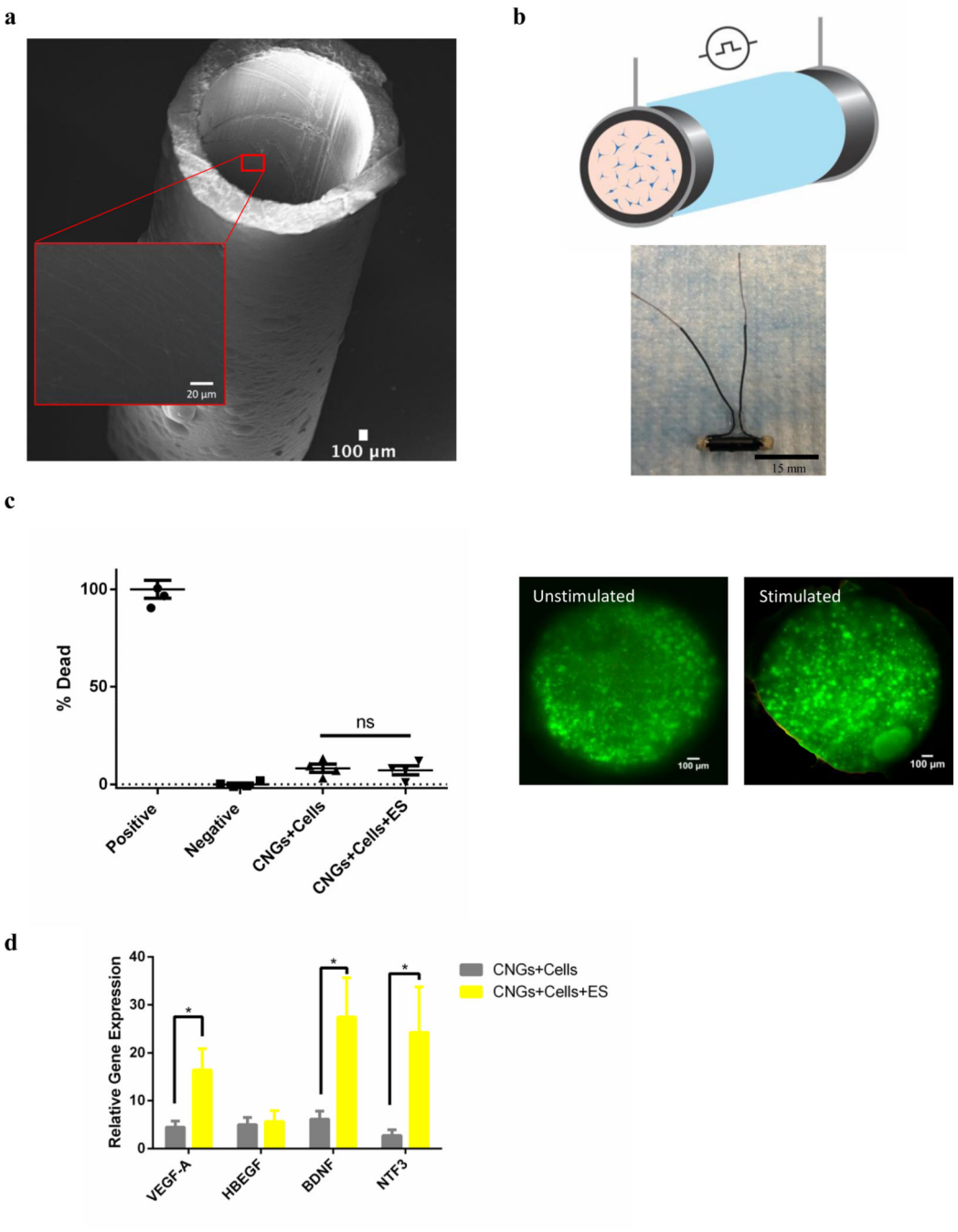

Fig. 1.

Electrical stimulation from CNGs maintains cell viability and upregulates the gene expression of neurotrophic factors in hNPCs. (**a**) SEM images of 3D CNGs made of polypyrrole. (Inner diameter: 1.63mm; Length: 15mm) (scale bar: 100 μm) (**b**) A cross-section schematic of CNG (black) that was insulated (light blue) for electrical stimulation (black circle) with hNPCs (blue) encapsulated in alginate (orange) (top panel). Longitudinal view of a CNG wrapped in insulation and attached with external wires for stimulation (bottom panel) (scale bar: 15mm). (**c**) Percentage of cell death quantified by the LDH assay

for unstimulated (CNGs+Cells) and stimulated hNPC-containing CNGs (CNGs+Cells+ES) after 1 day. The positive and negative controls were lysed cells and live cell culture on tissue culture plates, respectively (n=4) (left panel). Live/Dead staining of the hNPC-containing CNGs (green: live; red: dead) for unstimulated and stimulated groups (right panel) (scale bar: 100 μm). (**d**) The gene expression of vascular endothelial growth factor-A (VEGF-A), heparin-binding EGF like growth factor (HBEGF), brain-derived neurotrophic factor (BDNF), and neurotrophin-3 (NTF-3) for unstimulated (CNGs+Cells) and stimulated hNPC-containing CNGs (CNGs+Cells+ES) after 1 day. Comparing to hNPCs cultured on tissue culture plates, hNPC-containing CNGs showed gene expression of VEGF-A, HBEGF, BDNF, NTF3 were 4.47±1.28, 4.99±1.50, 6.13±1.69, 2.77±1.14 fold greater without electrical stimulation and 16.4±4.45, 5.65±2.28, 27.4±8.22, 24.2±9.51 fold greater with electrical stimulation, respectively. Incorporation of hNPCs into the CNGs upregulated the gene expression of VEGF-A, HBEGF, BDNF, NTF3 (CNGs+Cells). The addition of electrical stimulation further enhanced the expression level of VEGF-A, BDNF, and NTF3 (CNGs+Cells+ES) (n=4, *$p<0.05$). *Data were analyzed by the Student's t-test.*

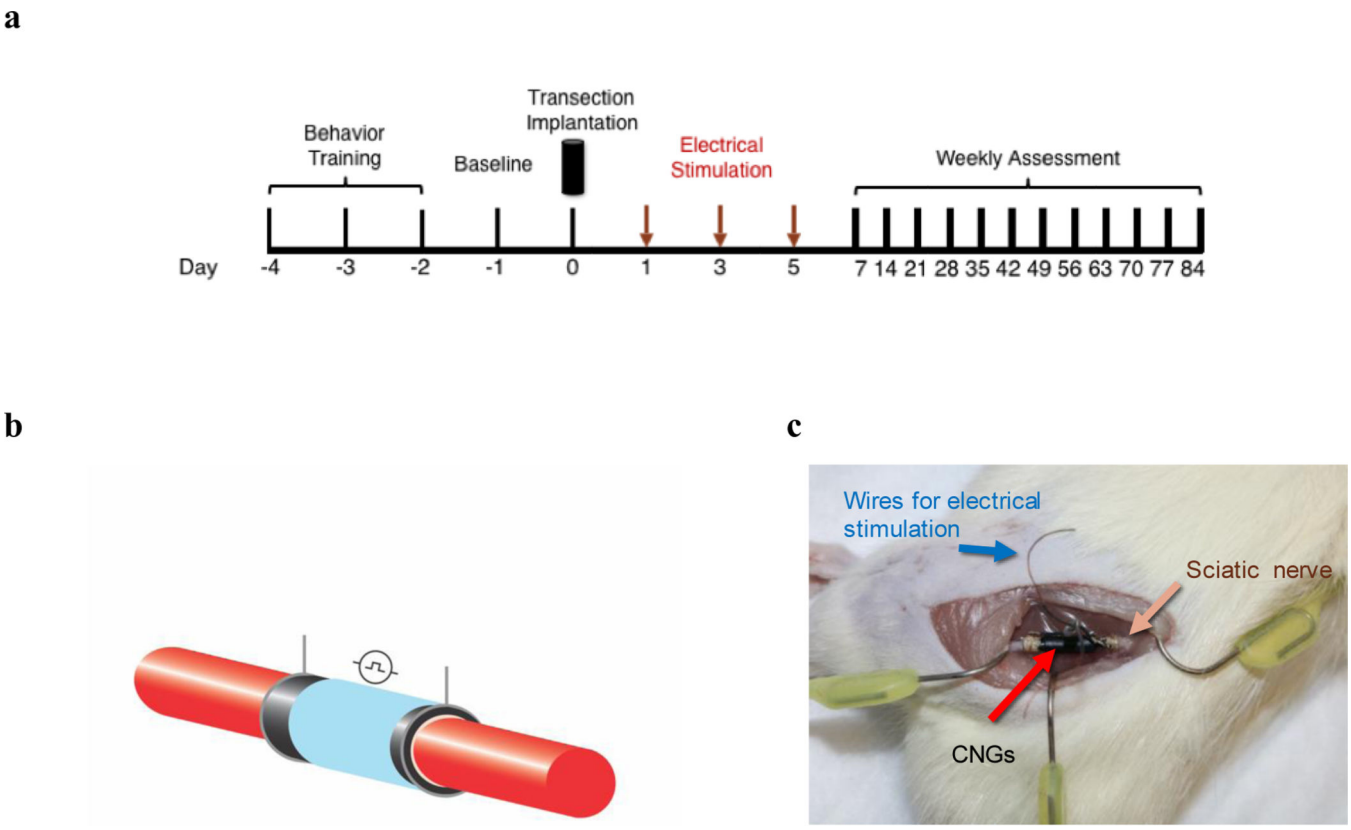

Fig. 2.

In vivo implantation of electrically-stimulated hNPC-containing CNGs. (**a**) Experimental timeline for implantation and subsequently animal behavior assessment. (**b**) A representative schematic of insulated CNGs bridging the transected sciatic nerve (red). (**c**) A picture of insulated CNGs implanted in a rat transected sciatic nerve model. The attached insulated wires were hidden under the skin where they could be retrieved for electrical stimulation.

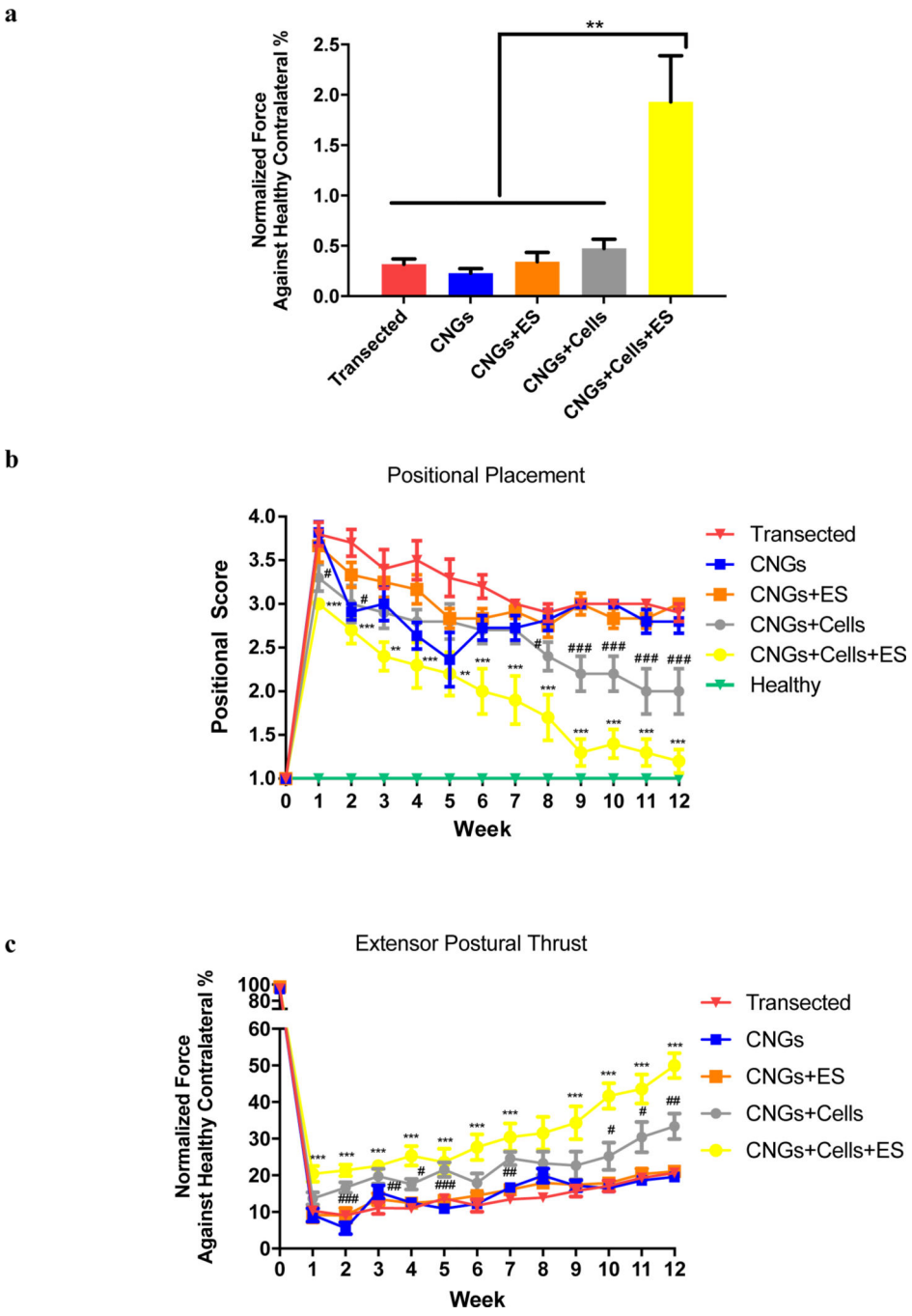

Fig. 3.

Electrically-stimulated hNPC-containing CNGs support functional recovery *in vivo*. (**a**) Electrically-stimulated hNPC-containing CNGs (CNGs+Cells+ES) show improved muscular gripping force compared to transected control (Transected), unstimulated CNGs (CNGs), stimulated CNGs (CNGs+ES), and unstimulated hNPC-containing CNGs (CNGs+Cells) after 12 weeks. Data were normalized against healthy contralateral sides of the animals. (n=10, **p<0.01) (**b**) Positional placement exhibited significant improvement in stimulated hNPC-containing CNGs (CNGs+Cells+ES) from week 1 onward. (**c**) Extensor postural

thrust showed that stimulated hNPC-containing CNGs (CNGs+Cells+ES) generated the most force from the injured leg compared to the transected group starting week 1. Data were normalized against the healthy contralateral sides. (n=10, # indicated “CNGs+Cells” group vs “Transected” control, * indicated “CNGs+Cells+ES” group vs “Transected” control, $p<0.05$, 0.01, 0.001 corresponding to the number of symbols, respectively) *For these graphs, data were analyzed by ANOVA followed by Tukey’s test per time point.*

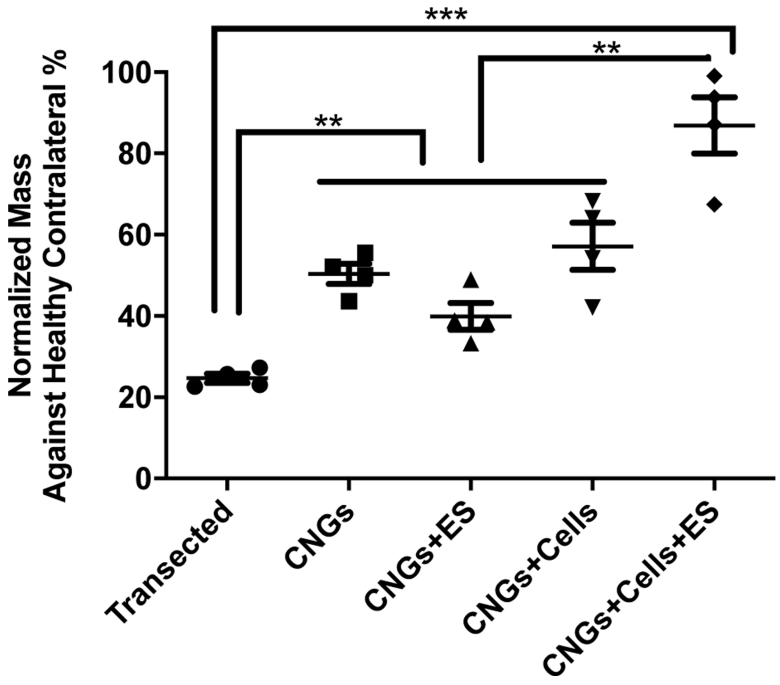

Fig. 4.

Electrically-stimulated hNPC-containing CNGs restore muscle mass. Gastrocnemius muscles that innervate with the sciatic nerves were harvested at the end of week 12. The stimulated hNPC-containing CNGs (CNGs+Cells+ES) retained a significant amount of muscle mass after successful nerve regeneration. Data were normalized against the healthy contralateral sides. (n=4, **p<0.01, ***p<0.001) *For these graphs, data were analyzed by one-way ANOVA followed by Tukey's test.*

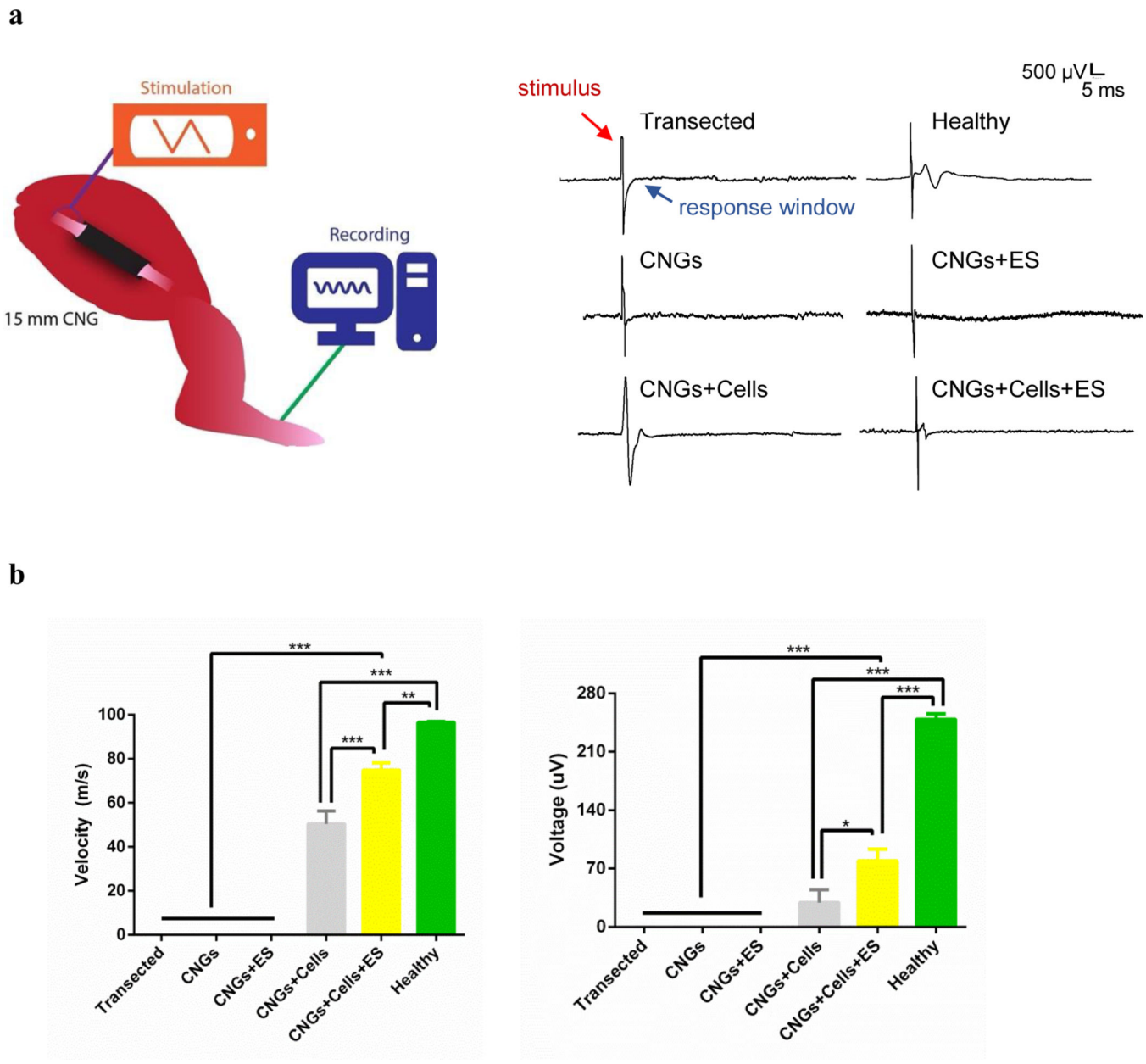

Fig. 5.

The electrophysiological analysis demonstrates functional recovery and reinnervation of regenerated sciatic nerves with their affected muscles. (**a**) A schematic showing the proximal stimulation of the sciatic nerve and recording of the compound action potential from the paw 12 weeks after CNG implantation (left panel). Following proximal stimulation, compound action potential was observed in the following groups: healthy control (healthy), unstimulated hNPC-containing CNGs (CNGs+Cells), and stimulated hNPC-containing CNGs (CNGs+Cells+ES). The transected control (Transected), unstimulated (CNGs) and stimulated CNGs (CNGs+ES) did not exhibit any signals following proximal stimulation (right panel). (**b**) The conduction velocity measured from the electrophysiology showed stimulated hNPC-containing CNGs (CNGs+Cells+ES) with the fastest nerve speed of the

experimental groups in response to stimulation (left panel). The stimulated hNPC-containing CNGs (CNGs+Cells+ES) also showed increased amplitude from compound action potential following proximal stimulation (right panel) (n=3, *p<0.05, **p<0.01, ***p<0.001). *Data were analyzed by one-way ANOVA followed by Tukey's test.*

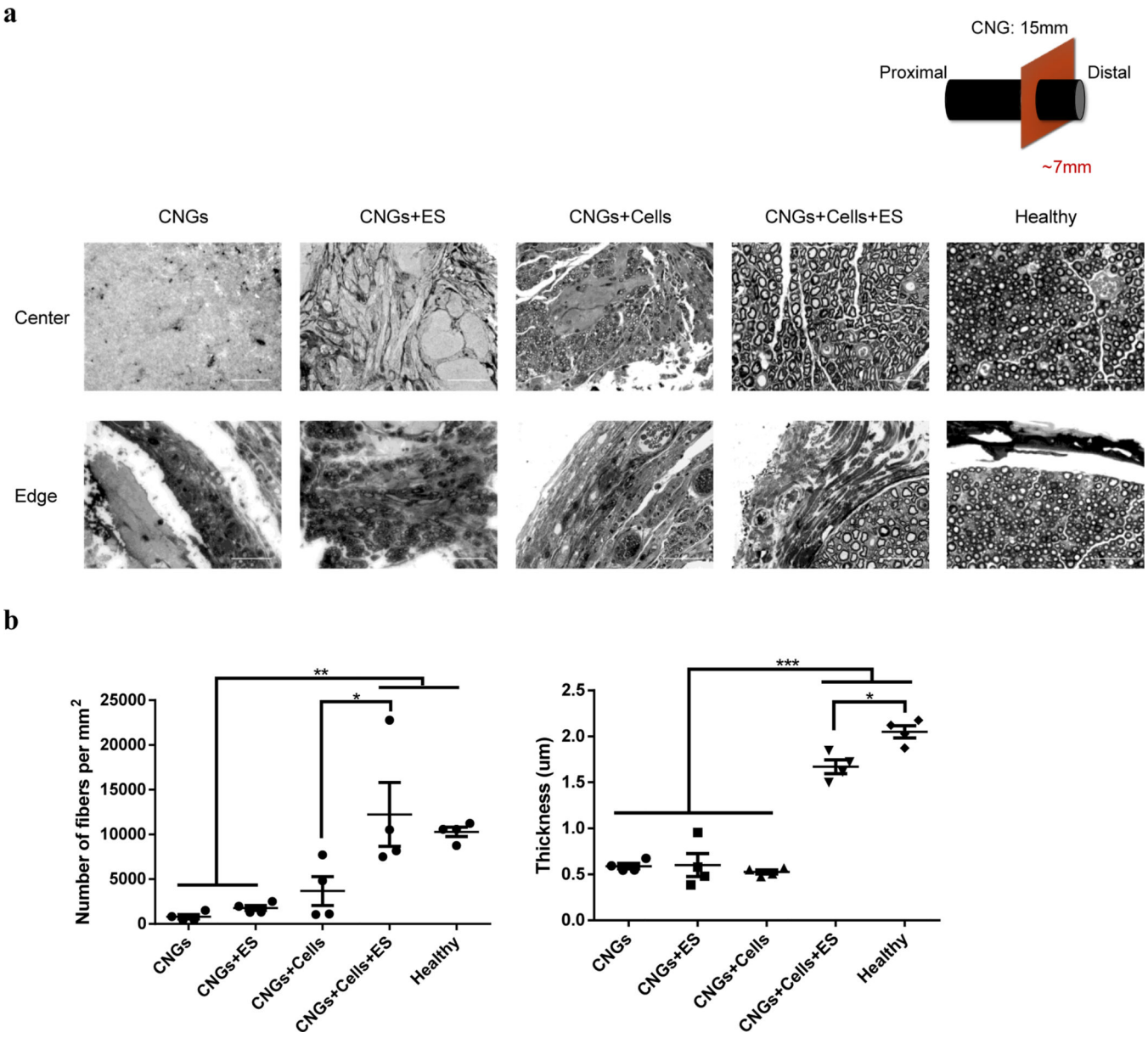

Fig. 6.

Electrically-stimulated hNPC-containing CNGs increase the number of myelinated nerve fibers with adequate myelination. (**a**) Stimulated hNPC-containing CNGs (CNGs+Cells+ES) presented a significant amount of myelinated fibers than unstimulated hNPC-containing CNGs (CNGs+Cells), unstimulated CNGs (CNGs), and stimulated CNGs (CNGs+ES) in both central and peripheral areas of the nerve conduits based on toluidine blue staining. (scale bar: 50 μm) (**b**) Electrical stimulation increased the number of axons and myelination thickness in the stimulated hNPC-containing CNGs (CNGs+Cells+ES). (n=4, *p<0.05, **p<0.01, ***p<0.001) *Data were analyzed by one-way ANOVA followed by Tukey's test.*

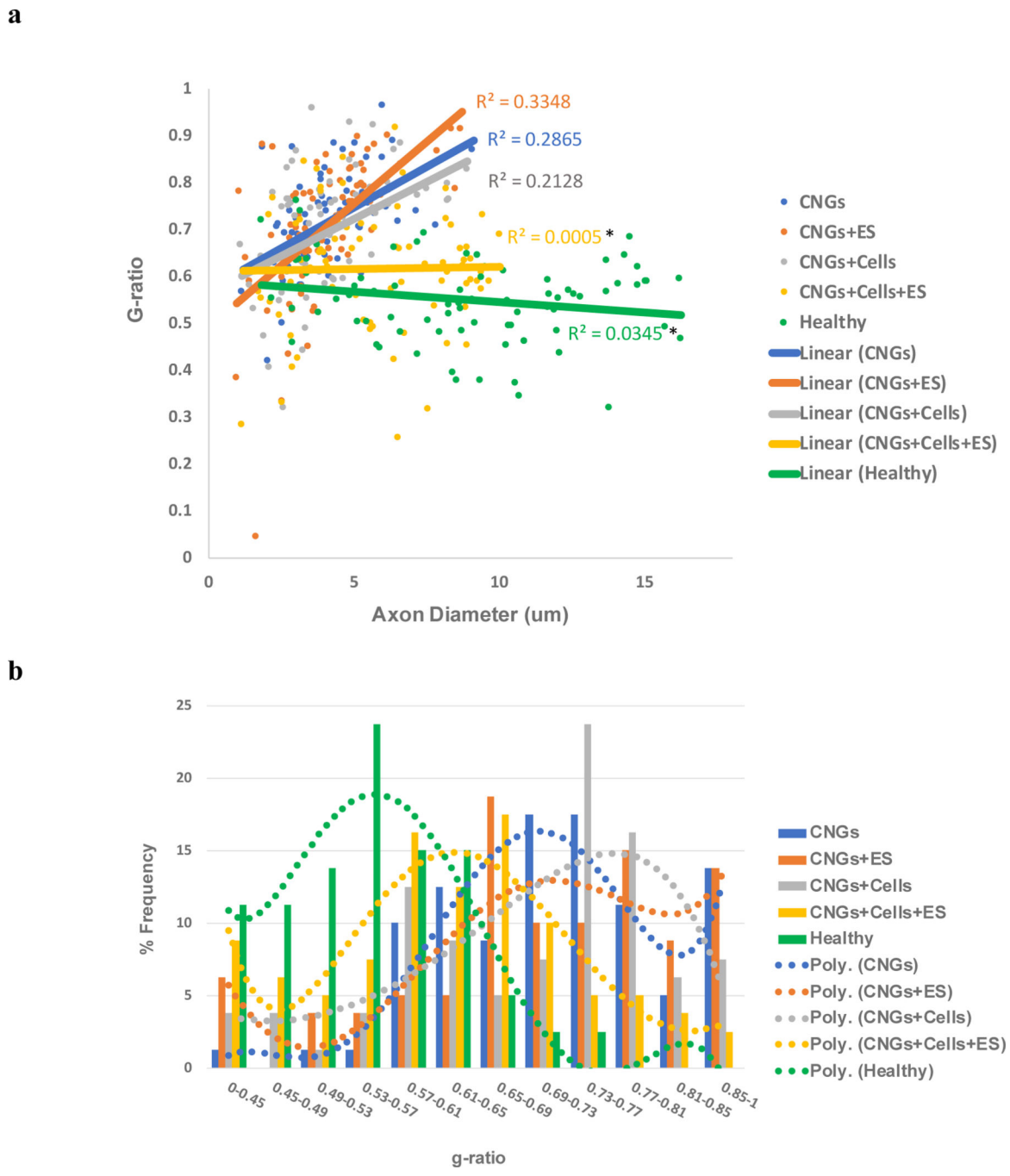

Fig. 7.

Electrically-stimulated hNPC-containing CNGs show improved g-ratio for sizeable nerves. (**a**) This diagram examines the relationship between axon diameter and g-ratio. The scatter plot displayed the g-ratio of individual myelinated axons (80 randomly chosen nerve fibers per group for n=4) as a function respective to the axon size. The linear regression of g-ratio measurement for unstimulated (CNGs) and stimulated CNGs (CNGs+ES), unstimulated (CNGs+Cells) and stimulated hNPC-containing CNGs (CNGs+Cells+ES), and healthy group (Healthy) was drawn. Stimulated hNPC-containing CNGs (CNGs+Cells+ES)

presented a g-ratio of ~0.6 and minimal variability (R^2=0.005) even for larger axons, followed by unstimulated hNPC-containing CNGs (CNGs+Cells), unstimulated CNGs (CNGs), and stimulated CNGs (CNGs+ES). The R^2 values of stimulated hNPC-containing CNGs (CNGs+Cells+ES) and healthy group (Healthy) were significantly different from the stimulated CNGs (CNGs+ES) (n=4, *p<0.05) (**b**) Based on the frequency histogram (80 randomly chosen nerve fibers per group for n=4), stimulated hNPC-containing CNGs (CNGs+Cells+ES) had most nerve fibers within a g-ratio range of ~0.61–0.65, which was closer to the frequency bin of ~0.53–0.57 in the healthy group (Healthy). The unstimulated hNPC-containing CNGs (CNGs+Cells) were within ~0.73–0.77, unstimulated CNGs (CNGs) were ~0.69–0.73, and stimulated CNGs (CNGs+ES) were ~0.65–0.69. Polynomial curves were fit with the frequency response bins. *Data were analyzed by one-way ANOVA followed by Tukey's test.*

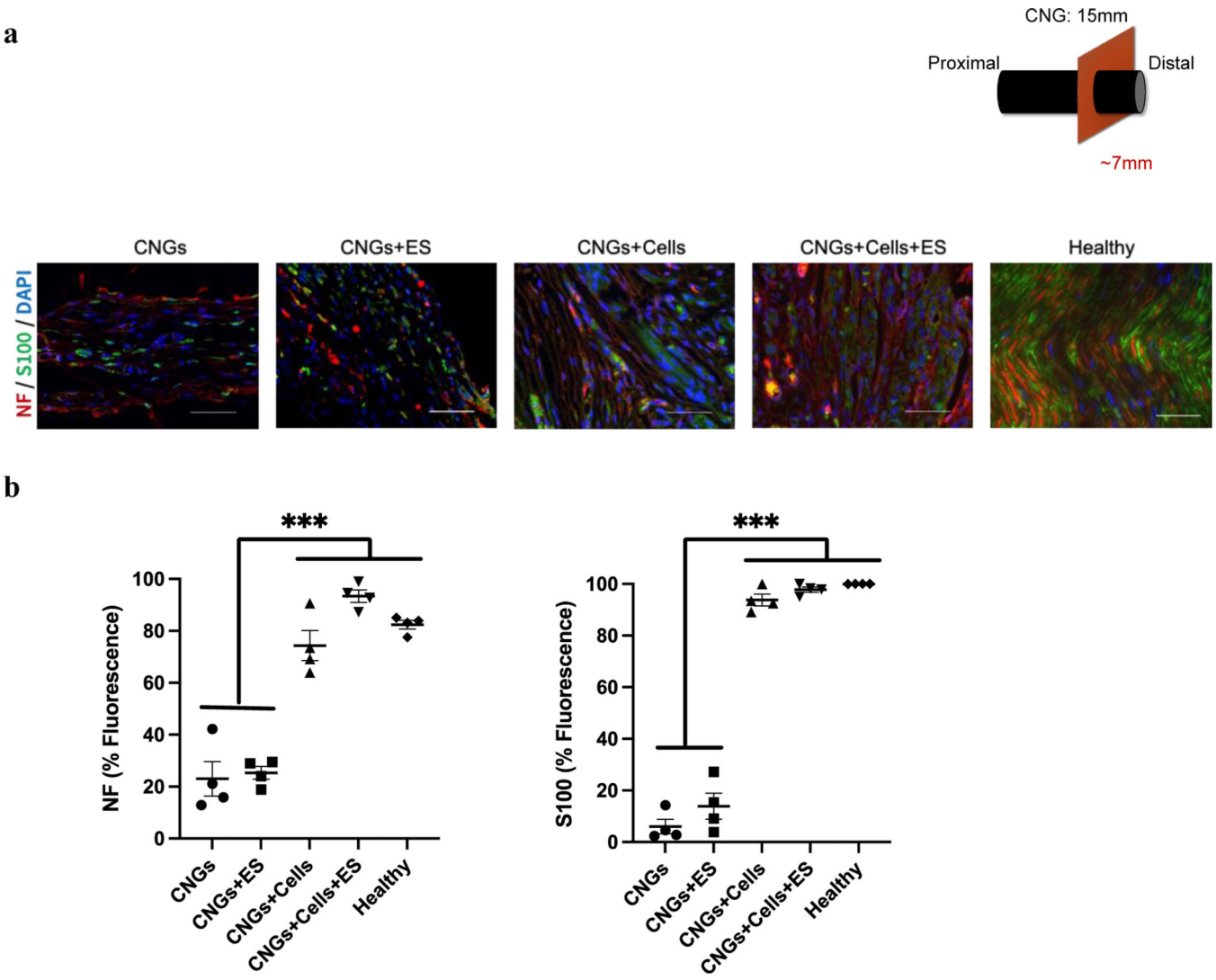

Fig. 8.

Both unstimulated and stimulated hNPC-containing CNGs demonstrates a high level of biomarkers: neurofilament (NF) for axons and S100 for Schwann cells. (**a**) Unstimulated (CNGs+Cells) and stimulated hNPC-containing CNGs (CNGs+Cells+ES) displayed more aligned axons (red) with Schwann cells (green) wrapping around the nuclei (DAPI: blue). The unstimulated (CNGs) and stimulated CNGs (CNGs+ES) presented fewer aligned axons with the scattered Schwann cell marker (scale bar: 50 μm). (**b**) Normalized fluorescent intensity showed a higher expression level of neurofilament and Schwann cells for unstimulated (CNGs+Cells) and stimulated hNPC-containing CNGs (CNGs+Cells+ES). (n=4, ***p<0.001) *Data were analyzed by one-way ANOVA followed by Tukey's test.*

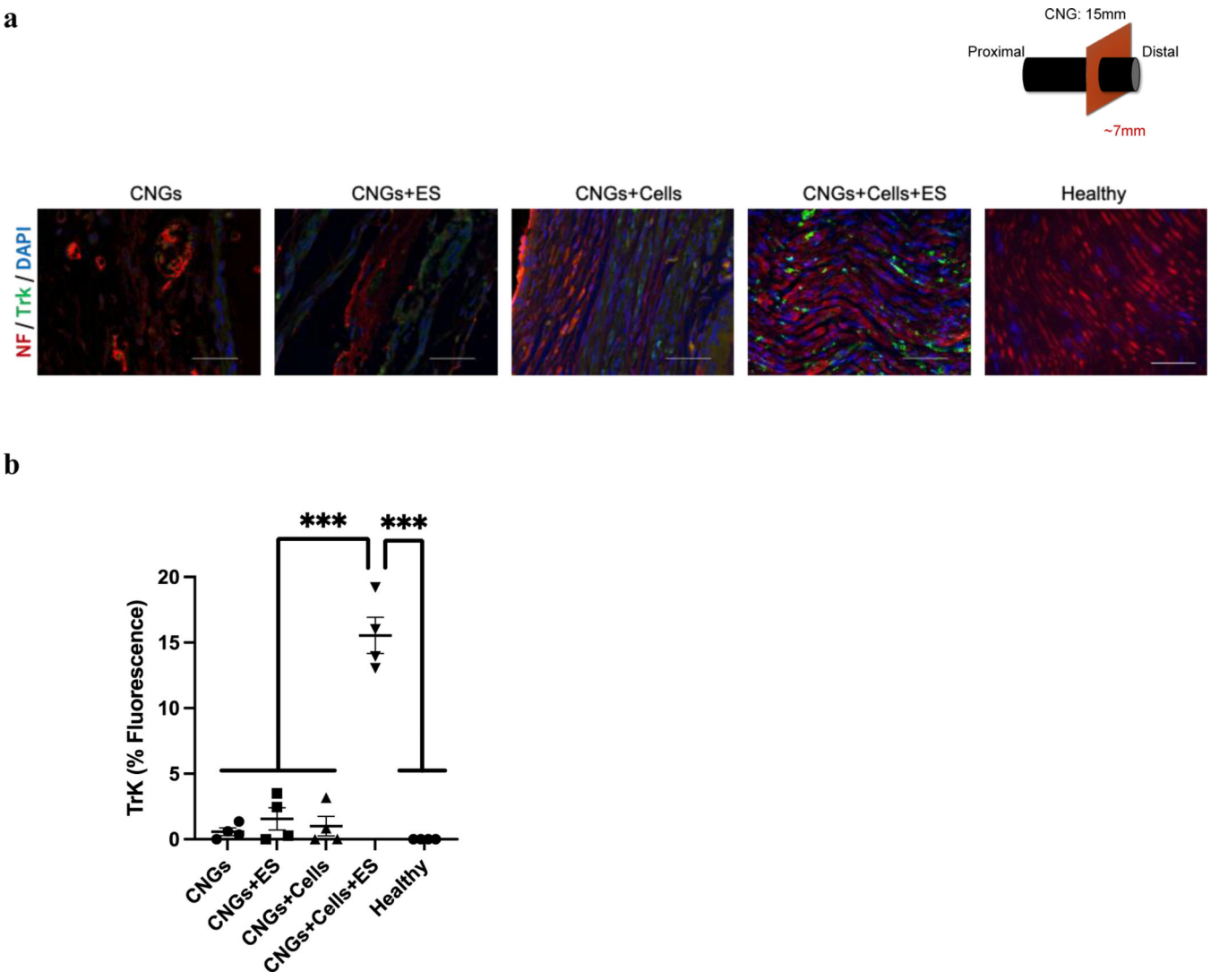

Fig. 9.

Electrically-stimulated hNPC-containing CNGs exhibit an increased level of Trk receptors on regenerated nerves. (**a**) Stimulated hNPC-containing CNGs (CNGs+Cells+ES) expressed Trk receptors at a higher level than unstimulated hNPC-containing CNGs (CNGs+Cells), unstimulated CNGs (CNGs), and stimulated CNGs (CNGs+ES) (scale bar: 50 μm). (**b**) The normalized fluorescent intensity showed that stimulated hNPC-containing CNGs (CNGs +Cells+ES) significantly enhanced the expression of Trk receptors. (n=4, ***p<0.001) *Data were analyzed by one-way ANOVA followed by Tukey's test.*